The Design and Application of a Nonlinear Series Compliance Actuator for Use in Robotic Arms

by

Arrin Katz

B.A.Sc. Engineering Science
University of Toronto, 1997

Submitted to the Department of Mechanical Engineering
in partial fulfillment of the requirements for the degree of

Master of Science in Mechanical Engineering

at the

MASSACHUSETTS INSTITUTE OF TECHNOLOGY

September 1999

Signature of Author.....
Department of Mechanical Engineering,
August 6, 1999

Certified by.....
Dr. J. Kenneth Salisbury, Jr.
Principal Research Scientist
Thesis Supervisor

Accepted by.....
Professor Ain A. Sonin
Chairman, Committee on Graduate Students

The Design and Application of a Nonlinear Series Compliance Actuator for Use in Robotic Arms

by

Arrin Katz

Submitted to the Department of Mechanical Engineering
on August 6, 1999 in partial fulfillment of the
requirements for the degree of Master of Science in
Mechanical Engineering

Abstract

The work presented here addresses the problem of providing robotic manipulators with improved force control and force sensing capabilities. A nonlinear compliant element for use in cable driven robotic manipulators was designed and built. The compliant element provides a nonlinear (exponential) force displacement behavior. This device is similar to the human hand in that it provides a large dynamic range (defined as the ratio between the largest exertable force and the smallest exertable force), near constant dynamic resolution, early contact detection and changing stiffness of the element. Additionally, the compliant element was designed with ease of manufacturability and assembly in mind and sensitivity for off the shelf components.

The effects of placing these compliant elements in line with a cable transmission system were investigated. System performance as a function of element preload was studied. Dynamic response for an open loop linear system equivalent was obtained and used to suggest controller designs. Using these suggested controller designs, the dynamic response of the nonlinear closed loop (position) system was observed.

A set of design requirements was developed and a compact design for the compliant element is presented. An experimental force displacement curve for the element was obtained and the position tracking performance of the actuator was evaluated.

Next, the compliant element was incorporated into the Compliant Arm Design for Digging (CADD), a 4 degree of freedom manipulator designed in collaboration with Andrew Curtis to examine the performance of the compliant elements in a 'real world' setting. The design presented in this work was incorporated into 2 degrees of freedom of the manipulator and the compliant element designed by Curtis was included in the remaining 2 degrees of freedom.

Thesis supervisor: J. Kenneth Salisbury
Title: Principal Research Scientist

Acknowledgements

I would like to thank my advisor Ken Salisbury for providing me the opportunity to work in such a great environment and explore freely for the past two years.

To my lab mates who made life at the lab enjoyable. Jesse who I could always count on to help, guide, hit the ball or just hang out, Brian for providing many helpful suggestions, Mark for laughing at my canuck jokes, eh!?, Andrew for making me serious once in a while and working together on the arm design, Don for countless hockey debates, and Ela for tolerating me for the past two years in the office.

To the great support staff in the AI lab, Ron Wiken for always helping out with suggestions, components and other random stuff. Jacqui Taylor for making sure I could order stuff. To Leslie, Joan and the ME grad office crew for making it such a pleasure to stop by.

To my mejor amigo, Luis, for all the encouragement, support and sarcasm over the years.

To my brother, Gady, for always making me laugh (at my own expense).

To my grandma Mia and the rest of the family for always going beyond the call of duty.

And last but not least, to my parents, Gaby and Carol, who sacrificed so much to give us endless opportunities, for their love and understanding.

Funding for this research was provided by NASA under contract number 959774, "Sample Acquisition, Grasping & Excavation (SAGE), Compliant Arm Design for Digging (CADD); & SSX Technology."

Table of Contents

Table of Figures

Chapter 1 – Introduction

This thesis addresses the design and construction of a manipulator for planetary geological exploration, in particular, the exploration of Mars. The current manipulator designs from NASA use highly geared motors in a non-backdrivable configuration. The main reason for using this type of arrangement is the severe limitation on weight, space, and power efficiency that are placed on space related components. While this design methodology yields a robust manipulator that can provide large torque using a relatively low weight actuator, it is severely limited in the tasks that it can perform.

Additional issues raised for planetary manipulators arise as a result of communication delays. The long time delay in signals transmitted between earth and Mars requires that any rover or manipulator be capable of some degree of autonomous maneuvering or manipulation. A key issue while providing autonomy to any manipulator is to ensure that it can interact safely with the environment so that the manipulator or the operational environments are not harmed. In order to provide this kind of protection, accurate sensing, detection, and application of the forces involved is required. To design a better manipulator, the advantages and disadvantages of the current available manipulator designs must be understood.

One advantage of the manipulators currently used by NASA/JPL is that they are robust and low weight. In order to achieve this low weight, the manipulators use highly geared electrical motors as actuators. As a result, the manipulators lack of a way to accurately measure forces and implement explicit force control. The reason that force control for the manipulator is desirable is that it allows the manipulator to apply and detect accurate forces on/from the environment. The manipulator's main goal is to perform sample acquisition tasks, however, the rate of performing science can be increased by gathering data while these tasks are in progress. The data could provide valuable information for determining soil composition and soil properties.

In order to obtain this additional useful geological data there is a need to be able to apply accurate repeatable forces and measure these forces. There are numerous ways to provide force control and force measurements for the system. Some manipulators use explicit force sensors that provide measurement of the force at the endpoint. One of the problems with force sensors is that they could be easily damaged if subjected to a shock load. Another method implemented on the Whole Arm Manipulator (WAM) robot (Salisbury, 1988) is the use of motor current sensing to detect force in the arm. An accurate measurement is dependent on backdrivability and a low back drive friction. A third more noble way is to provide a compliant transmission that could measure the forces that are applied by the manipulator by measuring the forces in the transmission (e.g. spring deflection measurement).

1.1 Force Control

The common view in the robotics community is that a good manipulator is a stiff manipulator. This notion is exemplified by the volume of papers describing methods to overcome compliance introduced by link or transmission flexibility. The desire for high stiffness is driven by the traditional factory floor robotic applications. These robots perform tasks that are predominately position control tasks of high precision. For those types of tasks, any reduction in stiffness results in bandwidth loss. The lowered bandwidth due to the reduced stiffness reduces the speed of operation of the manipulator and deteriorates its position tracking performance.

The main problem with this paradigm that 'stiffer is better' (Pratt, 1995a; Pratt 1995b) arises when the robot is required to perform manipulation tasks, that is interact with the environment. These are key tasks that are of interest in this research. The problem of interacting and applying forces on objects, or detecting contact with various environments, is intrinsically difficult when the transmission is stiff. The main difficulty follows from the fact that most manipulators use electric motors that have been geared in order to provide high forces at low speeds. As a result, a small manipulator motion results

in a large force. Additionally, the gearing of the motor introduces undesirable effects such as friction, backlash and torque ripple, which deteriorate the manipulator's ability to interact with environments and apply accurate, repeatable forces.

In order to be able to interact with various environments, there is a need to accurately control forces over a wide dynamic range. This need was recognized by researchers who have developed a few methods to address the issue. Initially, the force control problem was addressed by providing either active or passive force control. A general overview of the methodologies available for force control is found in Williamson's work (Williamson, 1995). More recently a different approach to the problem was undertaken. The idea that 'stiffness isn't everything' adds a spring, or a compliant element in series with the actuator. This compliant element provides shock load protection and essentially transforms the force control problem to a position control problem. While the bandwidth of the system is reduced, it is not critical for the task at hand. Recent communication with JPL point that the Mars polar lander arm (MVACS arm), a robotic arm on the current mission to Mars, isn't required to perform high speed manipulation. The manipulator moves at a rate of about $1\text{-}2^0$ per second, so a motion of 180^0 takes a few minutes to complete.

1.2 Previous Work

The idea of introducing compliance to a system to ease interaction with environments has been developed in the areas of both hardware and software. It was shown that the 'peg in the hole' problem is significantly simplified when some passive compliance is introduced to the manipulator (Whitney, 1982). From a software point of view there are many different methods of providing force control. Impedance control (Hogan, 1985), and hybrid force/position control (Raibert and Craig, 1981) are examples of software implemented force control. One of the problems with implementing force control and introducing compliance via software is the computational intensity associated with the control algorithms. In addition, these force control methods have the problem of

becoming unstable when contacting very stiff environments. One way to solve this problem was to lower the effective stiffness of the environment by providing rubbery coating to the fingers or contact area. This made the system more stable by compensating for errors in the model.

In their work Pratt and Williamson (Pratt, 1995a; Pratt 1995b) suggest that adding a spring in series with the actuator could improve manipulator force control performance. Using this series elastic actuator the force control problem is simplified to a position control problem reducing the complexity of associated control algorithms. Williamson demonstrated (Williamson, 1999) that several tasks (crank turning, sawing) that are difficult to implement with a traditional stiff manipulator without an accurate geometric model representation of the environment, become very easy with a compliant actuator. The spring actuator designed by Williamson (shown in Figure 1-1) is a constant stiffness torsion spring that uses a potentiometer and strain gauges to measure the deflection of the element and provide force measurements.

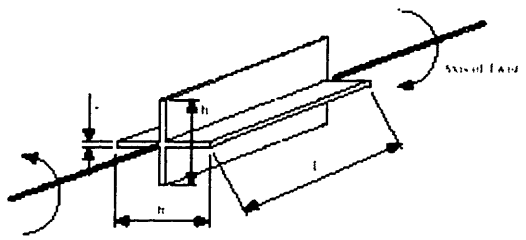

Figure 1-1: Compliant element designed by Williamson

Some work at the Leg Laboratory at MIT on walking robots also introduced compliance in series with the actuator. One of the robots, Spring Turkey, used constant stiffness extension springs in series with the cable transmission. Difficulties arose with this system due to extension of the springs beyond their elastic range and hence prompted an investigation into the use of compression springs whose deflection is limited by the bottoming out effect.

Shah (Shah, 1997) developed an exponentially compliant flexible coupling element that works in torsion as well. The benefit of this system over the previous systems described was that due to its exponential nature, it provided a constant force resolution over its entire dynamic range. Additionally, the element provided a dynamic range (defined as the ratio between the largest exertable force and the smallest exertable force) of 1000 which is about an order of magnitude better than could be achieved with normal manipulators (Morrell, 1996). The increased dynamic range is possible since initially, a small torque is required to produce a given deflection. As the overall deflection of the element increases, a larger torque is required to achieve the same additional given deflection. The spring elements used to obtain the variable stiffness for the system were Buna N rubber balls. The main drawback of this device was that the rubber ball characteristics would change over time and as a result, system performance and predictability would deteriorate over time.

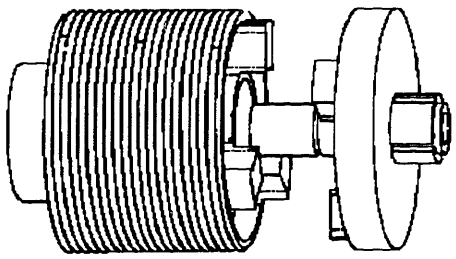

Figure 1-2: Compliant element designed by Shah

Some researchers investigated the effects of transmission stiffness using multiple actuators for every degree of freedom. Sugano (Sugano, 1992) suggested adding a spring to a finger tip and a brake mechanism to provide damping. The system has two independent actuators to control continuous variation of compliance and joint positioning.

Morrell (Morrell, 1996) tested out the micro-macro actuator with various values of transmission stiffness to provide force control. A dynamic range of about 800 and a bandwidth of nearly 60 Hz were achieved in this configuration. Morrell makes an interesting observation justifying the need for a nonlinear stiffening transmission. Low

stiffness and low impedance are most important when a manipulator initially makes contact. As the contact force becomes larger, a stiffer transmission is desired.

While the idea of using two actuators to provide improved force control performance and improved dynamic range is technically interesting, the likelihood of using it in a space application is low. The strict weight and power budgets would prohibit the use of an extra actuator for every degree of freedom.

1.3 Scope of Investigation

To address the problem of providing a robotic manipulator with improved force control and force sensing capabilities, a nonlinear series compliance actuator (NSCA) to be used in cable driven robotic manipulators was designed and built. The NSCA consists of an electrical motor and two compliant elements placed in line with a cable transmission drive.

The compliant element has a desired nonlinear (exponential) force displacement behavior. This device is similar to the human hand in that it provides a large dynamic range (defined as the ratio between the largest exertable force and the smallest exertable force), near constant dynamic resolution, early contact detection and changing stiffness of the element. Additionally, the compliant element was designed with ease of manufacturability and assembly in mind and sensitivity for off the shelf components.

The effects of placing these compliant elements in line with a cable transmission were investigated. System performance as a function of element preload was studied. The frequency response of an open loop linear system equivalent was obtained and used to suggest controller designs. Using these suggested controller designs, the dynamic response of the nonlinear closed loop system was observed.

A set of design requirements was developed and a compact design for the compliant element is presented. An experimental force displacement curve for the element was obtained and the position tracking performance of the actuator was evaluated.

Next, the compliant element was incorporated into the Compliant Arm Design for Digging (CADD), a 4 degrees of freedom manipulator designed in collaboration with Andrew Curtis to examine the performance of the compliant elements in a 'real world' setting. The design presented in this work was incorporated into 2 degrees of freedom of the manipulator and the compliant element designed by Curtis was included in the remaining 2 degrees of freedom.

1.4 Review of Thesis Contents

The thesis is organized as follows:

Chapter 2 describes theoretical models for predicted system behavior of the compliant element. These include the force displacement characteristics of the compliant element. The effects of placing the compliant elements in line with the cable transmission on the torque displacement characteristics and the effects of element preload on element performance. A simplified linear model of the system is examined and performance of the system is evaluated.

Chapter 3 discusses the design of the compliant element used in the nonlinear series compliance actuator. It defines the design requirements for the system and describes some of the design issues. In addition, experiments were performed to verify the predicted system performance presented in Chapter 2. Experimental results for force displacement characterization and position tracking for the system are shown.

Chapter 4 describes the design of the CADD that incorporates the NSCA developed in this research. Workspace considerations for the manipulator and forward kinematics are presented. Singular configurations are shown.

Chapter 5 provides conclusions and recommendations for further work and research.

Chapter 2 – Control and Modeling of the Nonlinear Series Compliance Actuator

2.1 Introduction

This chapter describes some of the theory behind the model of the NSCA and the characteristics of the compliant element. The effects of placing the compliant element in line with a cable transmission are examined as well as the effects of preload tension on device sensitivity.

The compliant element designed in this thesis was selected to provide compliance in the cable rather than a coupling that is attached to the motor. The desire is to compare the performance of this type of actuator (dynamic range, force resolution, etc.) to coupling style compliant actuators developed by other researchers and to the one that is currently designed by Andrew Curtis in our lab.

A conical compression spring was chosen as the mechanism to provide the nonlinear compliance. It was chosen over other options since it allowed for a compact method of obtaining these desirable characteristics (dynamic range, early contact detection, changing stiffness and near constant dynamic resolution), it was available as an 'off the shelf' component and it allowed for a minimal part count. A description of the force displacement characteristics of conical compression springs follows. The effects of placing these elements in line with a cable transmission are quantified and dynamic system response is evaluated.

2.2 Force displacement curve for conical compression springs

In order to understand the performance of the actuator, an initial model of the compliant element behavior was constructed. To provide a nonlinear stiffening transmission, the

desired force displacement curve for this element was exponential. This force displacement curve was chosen to help the compliant element mimic the reasons that human hands exhibit dexterity by providing a constant force resolution over the entire dynamic range and early contact detection.

In a stiffening element utilizing a conical compression spring, early contact detection is possible as a result of the low initial stiffness. A small initial force is needed to provide a noticeable spring deflection. The large dynamic range is achievable since the spring stiffens with an increased applied load, resulting in a larger load required to produce a given deflection. These characteristics are a result of the variable stiffness of the spring that can be explained using the stiffness formula for a regular spring.

The stiffness or spring rate of a normal compression spring is governed by the following equation:

$$R = \frac{G * d^4}{8 * n * D^3} \tag{2.1}$$

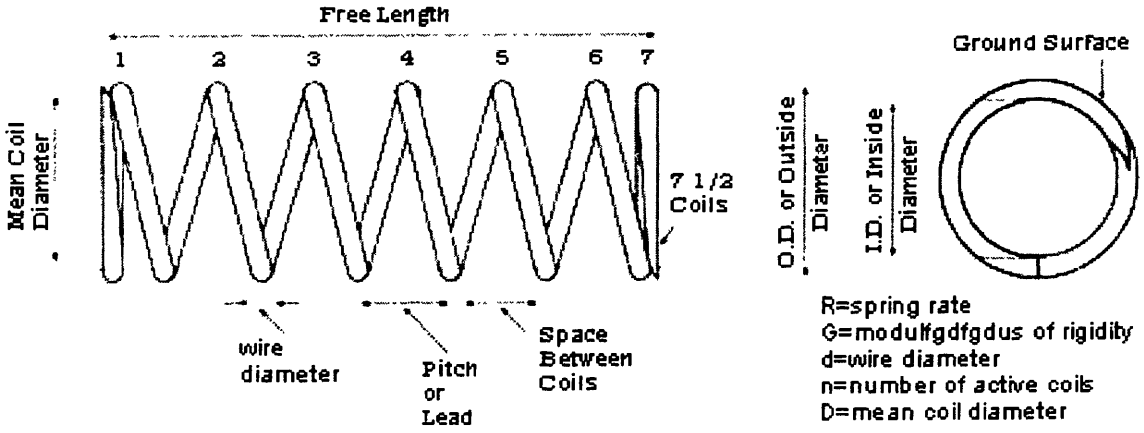

Figure 2-1: Spring parameters

It can be seen that in order to achieve variable stiffness there are several parameters that can be modified. A different material can be used, a change in wire diameter or a change in the coil diameter can be introduced. Out of these possible modifications, the easiest one to implement in one continuous spring is the change in coil diameter. A search of available springs showed that there are several types of springs manufactured that have a variable coil diameter. One such type of spring is the conical compression spring. Its main use is as replacement for compression springs since it provides better lateral stability and a lower tendency to buckle than regular compression springs. Additionally, due to its unique geometry it provides physical limits on travel and avoids permanent deformation, which would deteriorate the performance.

Figure 2-2: Conical compression spring

The conical compression springs are useful in our task since they have stiffening characteristic which is explained next. As with any system, the lowest stiffness elements are the first ones to deflect. In the conical compression springs, these correspond to the large diameter coils that are first to compress under an application of a load. After a certain load, the coils begin to bottom out. As these coils bottom out, the lower diameter, higher stiffness coils compress, hence requiring a larger force to provide the same motion that was required to compress the larger diameter coils.

This intuitive description of the stiffening characteristics of the spring is validated by a number of methods. A force deflection curve for the spring is found in Wahl (Wahl, 1963). As expected, the spring exhibits a stiffening characteristic as is shown in Figure 2-3.

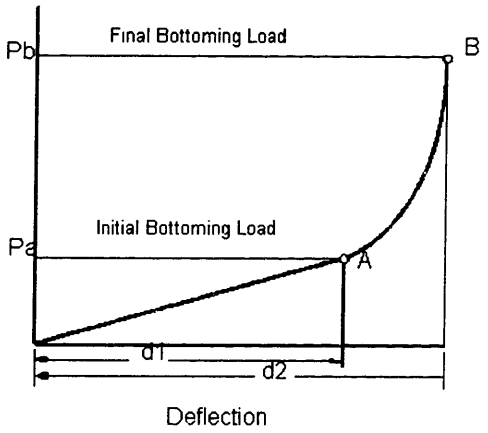

Figure 2-3: Force displacement curve for a conical compression spring

Up to point A, the initial bottoming out point, the spring behaves like a constant stiffness spring. After point A, the decreased coil diameter and the bottoming out effects contribute to the stiffening behavior described earlier.

A second method to predict the force displacement curve was to construct a piecewise linear spring model using a MATLAB simulation. This model (see Appendix A) assumes that the spring is made up of a combination of single turn springs with each single turn spring having a decreased diameter and as a result increased stiffness. As each spring bottoms out (based on the pitch value), the next coil becomes the active one resulting in increased stiffness. The model ignored the friction between the coils as they compress which serves to accelerate the stiffening behavior. Simulation results for TA-2364 spring are shown in Figure 2-4, and parameters for the TA-2364 spring are shown in Table 2-1.

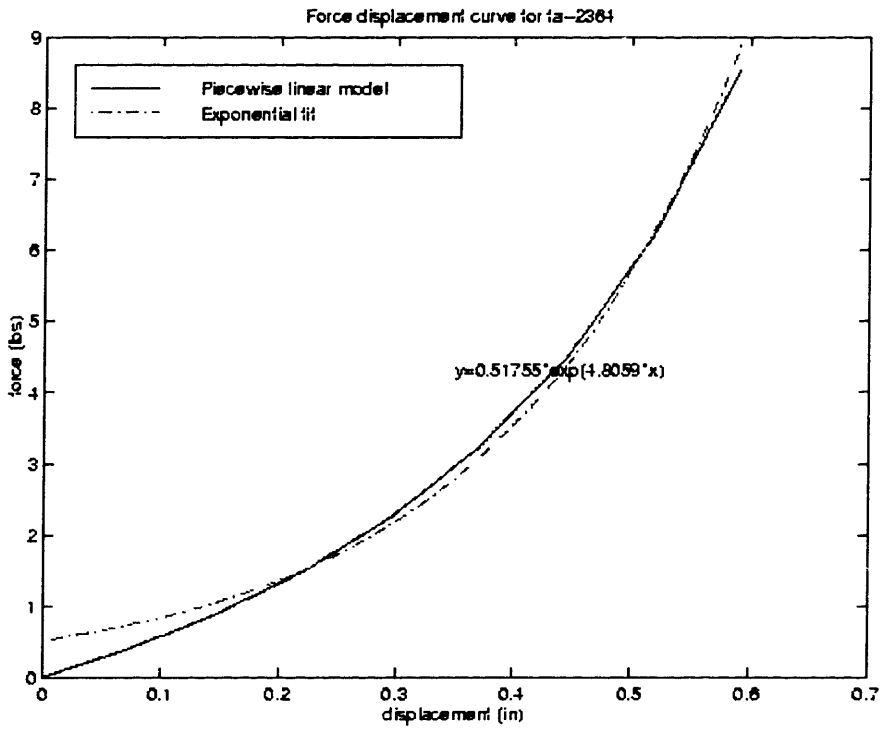

Figure 2-4: Force displacement curve for the conical compression spring TA-2364, simulation results

O.D.	0.297"x0.609"
I.D.	0.195"
Free Length	1.00"
Wire Diameter	0.051"
Total Coils	8.00
Material	Stainless Steel

Table 2-1: TA-2364 Spring specifications

A third method to verify the spring behavior attempted to develop a finite element model. However, due to the complex geometry of the spring, an accurate model representation was not achieved.

2.3 Cable preload effects and Torque displacement curve for the NSCA

Next, the compliant element previously described is placed in line with a cable transmission and the torque displacement characteristics are evaluated. Two compliant elements are required for every degree of freedom of the system, one is placed on the tension side and one on the slack side of the cable. The placement of the elements in line with the cable transmission affects the torque/force displacement characteristics of the system. A generic cable transmission system is shown in Figure 2-5. The transmission of torque in the system is due to the difference in tension between the slack and tension sides of the cable. With the introduction of compliant elements on both the tension and slack side of the system, the force differences between the two cable sides are more significant than in normal cable driven systems.

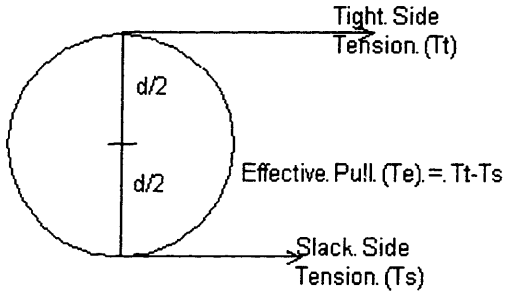

Figure 2-5: Torque transmission in cable systems

We start by examining the problem of torque transmission in a generic cable drive system. The torque for the system is defined by the following equation:

$$\tau = \frac{d}{2} * (T_t - T_s) \tag{2.2}$$

The equation shows that the dynamic range of the system is dependent on the force in both the tension and slack side. A key concern for this design is the effect of the preload on system performance. The minimal amount of preload force required should be

applied to the system. This is due to the fact that the most sensitive range of the device is at low displacements. As preload pushes the set point 'up' the force displacement curve, the dynamic range of the system and device sensitivity deteriorate.

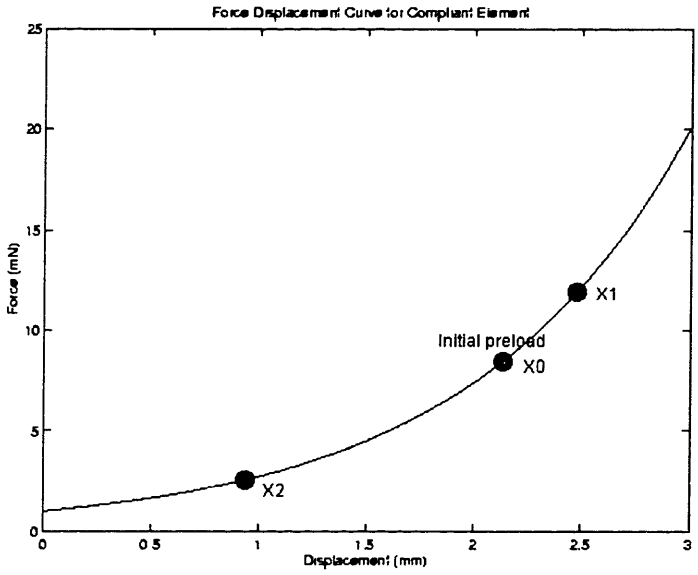

Figure 2-6: Preload settings for TA-2364 spring

We investigate the effects of preload on system performance. Initially, when there is no torque applied by the system, the following equation holds true:

$$\tau = 0, \quad T_t = T_s \tag{2.3}$$

Once a torque is applied,

$$\begin{aligned} T_{t-new} &= T_t + \Delta T, \\ T_{s-new} &= T_s - \Delta T \end{aligned} \tag{2.4}$$

and,

$$\tau = \frac{d}{2} * (T_{t-new} - T_{s-new}) = d * \Delta T \tag{2.5}$$

on the tension side,

$$\Delta T = a * e^{b*x_1} - a * e^{b*x_0} \tag{2.6}$$

and on the slack side,

$$\Delta T = a * e^{b*x_0} - a * e^{b*x_2} \tag{2.7}$$

from these expressions we can derive the following expressions for x_1 and x_2,

$$x_1 = \frac{1}{b} * \ln(\frac{\tau}{a*d} + e^{b*x_0}) \tag{2.8}$$

and,

$$x_2 = \frac{1}{b} * \ln(2 * e^{b*x_0} - e^{b*x_1}) \tag{2.9}$$

Using these equations, it is now possible to examine the torque displacement relationship of the compliant elements and study the effects of preload on the system performance.

It is known that for cable driven systems, in order to avoid slack in the cable it is desired to preload the cable to half the maximum force that it will experience. The same holds true for this system. Figure 2-7 shows the effects of varying the preload force on the torque-displacement curve of the system.

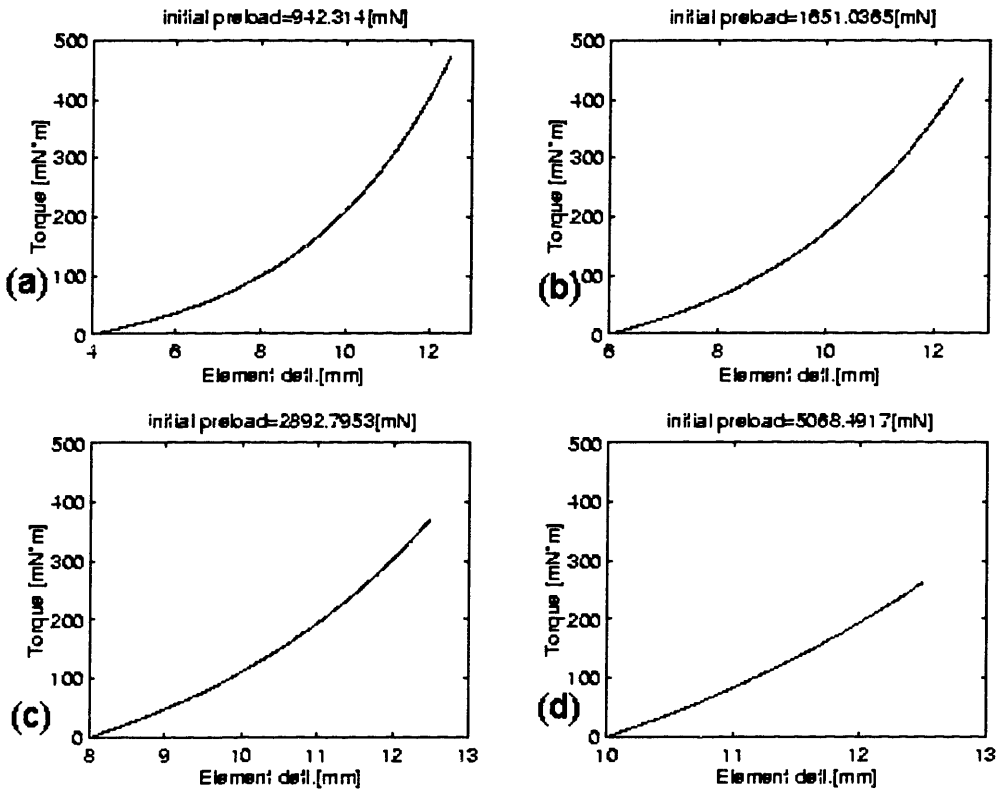

Figure 2-7: Effects of spring preload on torque-displacement curve. Preload force (a) 0.94[N], (b) 1.65[N], (c) 2.89[N], (d) 5.09[N]

The results show that as the preload force is increased, the initial slope of the torque-element deflection increases as well. This translates into lowered sensitivity of the system as a larger force is required to produce the same observable motion. As a result, it is best to use the lowest allowable preload force to minimize performance deterioration. One advantage of the system preload is that by moving the set point 'up' the compliance curve, the torque curve is strictly exponentially compliant and does not go through the linear section of the force displacement curve.

2.5 Single Axis Model of the NSCA

In order to examine the dynamic system performance, a single axis model of the nonlinear series compliance actuator was analyzed. This model is shown in Figure 2-8. Shown are the motor mass, mr_1, the compliant element with its associated stiffness and damping, k-element and b-element respectively, the link mass, mr_2, and the environment stiffness, k-environment.

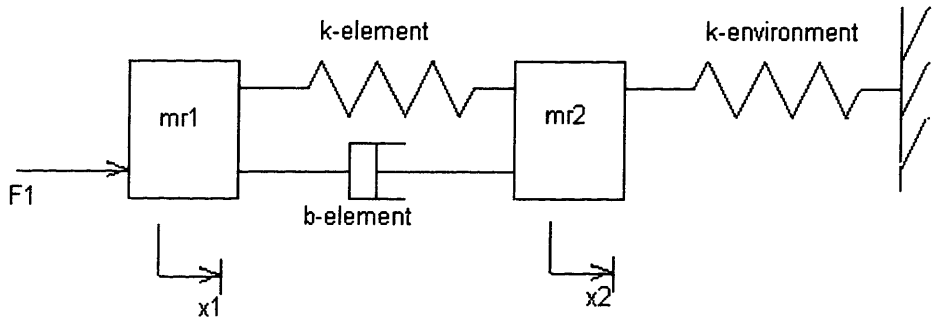

Figure 2-8: Simplified system model of the NSCA

The following equations describing system behavior can be written from Figure 2-8:

$$\begin{aligned} mr_1 * \ddot{x}_1 &= F_1 - a * e^{c*(x_1 - x_2)} - b_{elem} * (\dot{x}_1 - \dot{x}_2) \\ mr_2 * \ddot{x}_2 &= a * e^{c*(x_1 - x_2)} + b_{elem} * (\dot{x}_1 - \dot{x}_2) - k_{env} * x_2 \end{aligned} \tag{2.10}$$

where the nonlinear spring is described via the following relationship:

$$F_{spring} = a * e^{c*x} \tag{2.11}$$

This single axis model assumes that the motor is acting as a position source. The model completely neglects backlash in the gearhead, friction in the motor and the gearhead, and compliance of system components such as the cable. Based on this nonlinear model, a simplified linear model is presented next.

2.6 Simulation of NSCA Linear System Equivalent Dynamic Response

In order to test out the frequency response of the system, the model presented above was further simplified. The model assumes a linear spring and yields the following system equations:

$$\begin{aligned} mr_1 * \ddot{x}_1 &= F_1 - k*(x_1 - x_2) - b_{elem}*(\dot{x}_1 - \dot{x}_2) \\ mr_2 * \ddot{x}_2 &= k*(x_1 - x_2) + b_{elem}*(\dot{x}_1 - \dot{x}_2) - k_{env} * x_2 \end{aligned} \tag{2.12}$$

The output for the system is taken to be x_2 (link motion) and the effect of input F_1 on that output is evaluated. A range of values of k_{env} are tested to simulate different environments the manipulator makes contact with. An environmental stiffness of zero corresponds to the manipulator moving through free space. From the above equations, the following transfer function for the system is obtained:

$$\frac{X_2(s)}{F_1(s)} = \frac{b*s + k}{s^4*(m_1*m_2) + s^3*b*(m_1+m_2) + s^2*(m_2*k + m_1*(k+k_{env})) + s*(b*k_{env}) + (k*k_{env})} \tag{2.13}$$

Figures 2-9, 2-10 and 2-11 show the frequency response of the system with various environmental contacts. As can be seen from the figures the system has different dynamics when it is contact with an environment as opposed to moving in free space. The main difference can be deduced from the transfer function where a quick glance reveals that when this fourth order system is moving through free space it has a double integrator. The resulting -180^0 phase shows that the open loop system is unstable (or marginally stable) at low frequencies. As a result, a controller (e.g. PD controller) which adds phase is required to make the closed loop system stable. It is also interesting to note that the bandwidth for the system is reduced for the system interacting with the stiff environment.

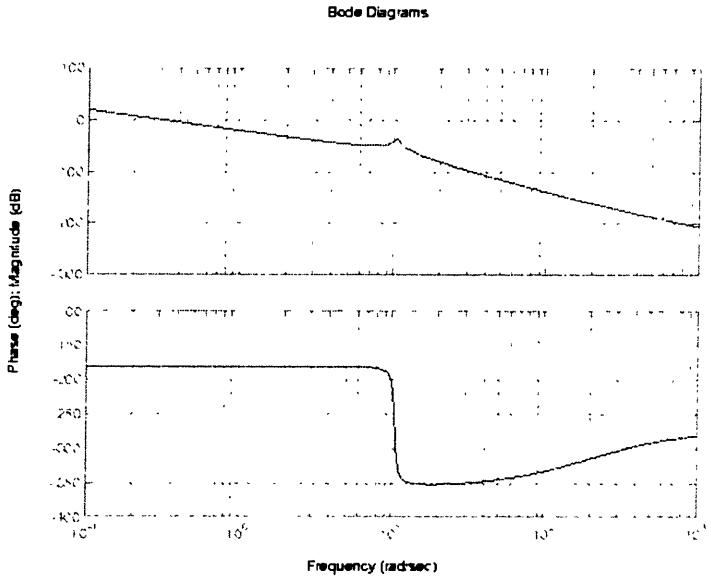

Figure 2-9: Frequency response for NSCA moving through free space

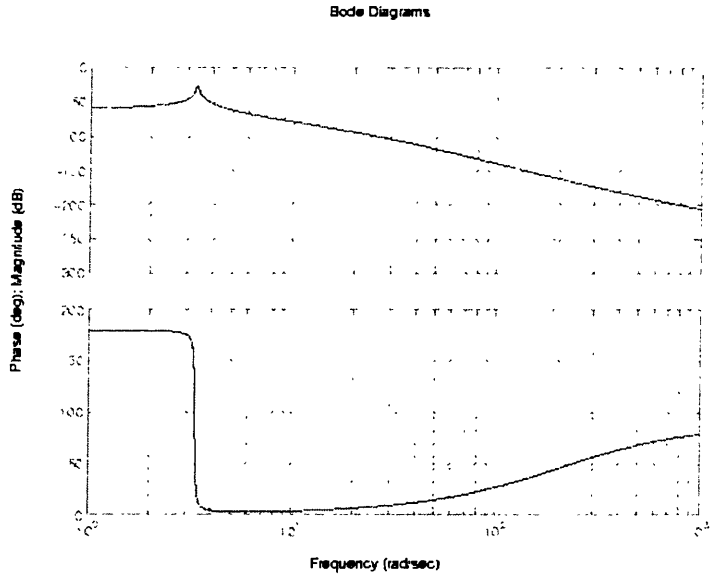

Figure 2-10: Frequency response for NSCA contacting a hard environment

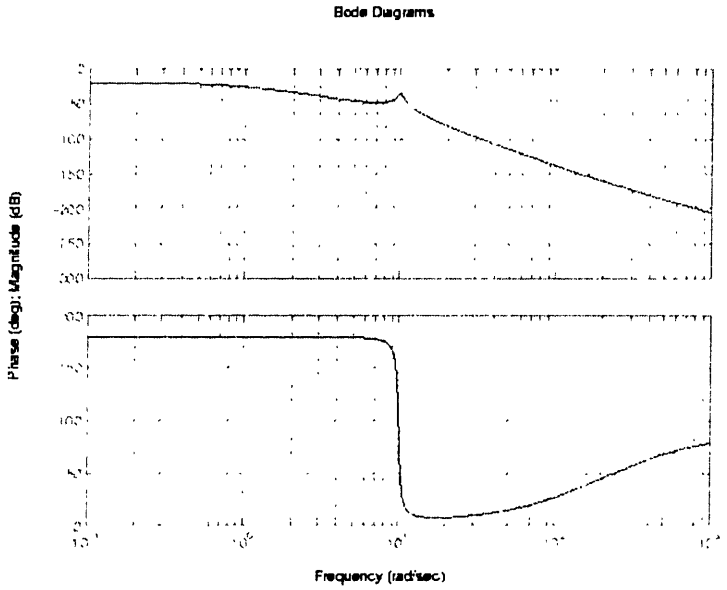

Figure 2-11: Frequency response for NSCA contacting a soft environment

2.7 Simulation of NSCA Closed Loop Dynamic Response

Based on the dynamic response of the linear model, an initial controller choice is implemented to obtain dynamic response for the closed loop nonlinear system. In order to evaluate the dynamic response of the closed loop nonlinear system, a Simulink model (see Appendix B) was assembled. This model is based on equation 2.12. A PD controller is implemented with gains K_p and K_v, representing proportional and velocity gains respectively. Desired input trajectory and a desired velocity in the form of sine waves of varying frequencies are provided to the system and the resulting output link motion is observed. In order to gain some insight to the performance of the nonlinear system, the effects of varying the motor inertia and the link inertia were studied.

Simulation results for the nonlinear close loop system are shown in Figures 2-12, 2-13, and 2-14. These frequency response plots show that the system behaves in a similar manner to the equivalent linear system. As the mass of the end point, m_2 is decreased, the bandwidth of the system increases. Also, the value of m_2 plays an important role in the

damping of the system. As the value of m_2 increases, the system becomes more and more damped as can be seen from the lack of overshoot in Figure 2-13.

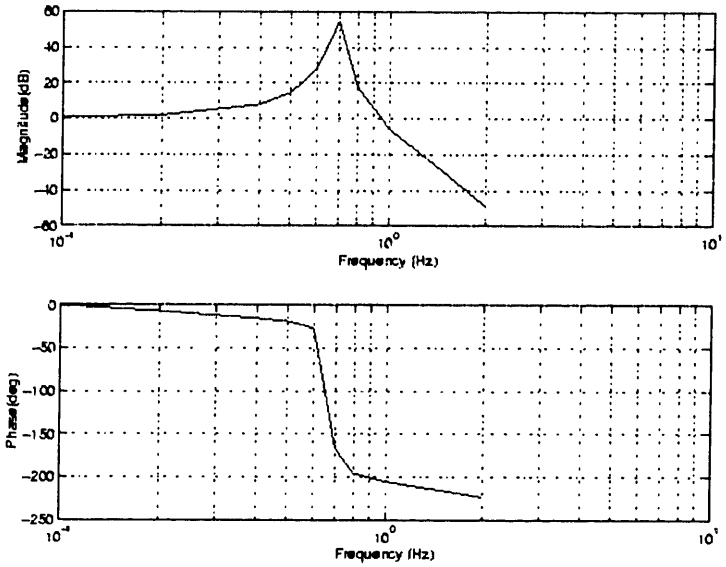

Figure 2-12: Frequency response of closed loop system with $m_2=0.1m_1$

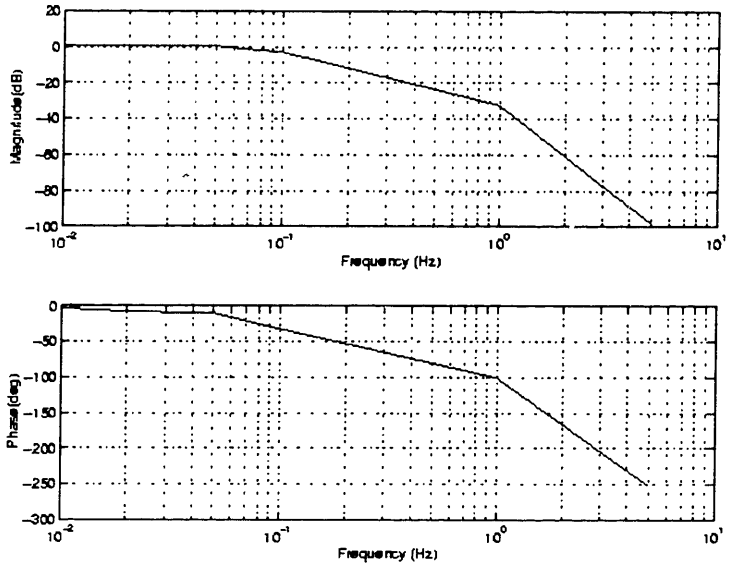

Figure 2-13: Frequency response with $m_2=10m_1$

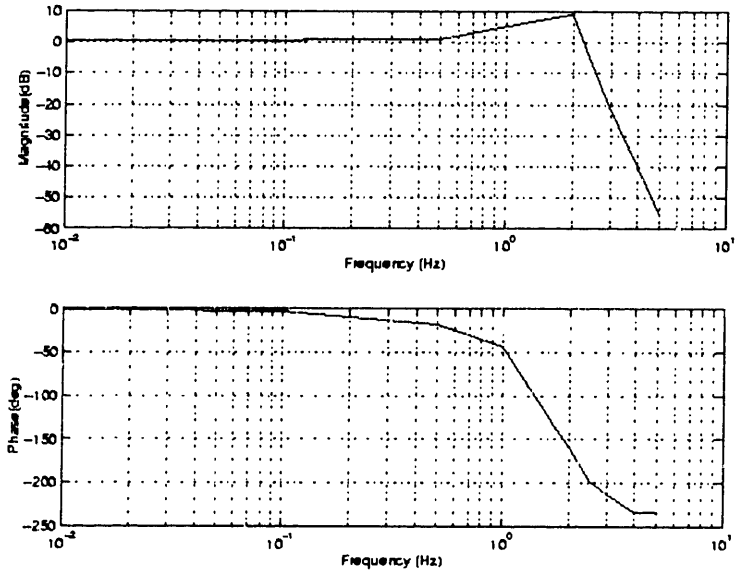

Figure 2-14: Frequency response of closed loop system with $m_2=m_1$

Chapter 3 - Compliant Element Design and Testing

3.1 Introduction

This chapter presents the design of the compliant element used in the NSCA. Design requirements are developed for the system and the design of the compliant element is described. Experiments to produce the force displacement curve are conducted and dynamic response of the system is evaluated.

3.2 Design Requirements

This work set out to design a compliant element that would allow robotic manipulators to achieve a better dynamic range, provide a constant force resolution across the dynamic range and give accurate contact sensing. The nonlinear stiffening behavior of the compliant element allows for these characteristics.

This type of element is different than the compliant actuators previously by other researchers since it will have the compliant element placed on the cable itself rather than an element that is attached directly onto the motor shaft (Williamson, 1995; Shah, 1997). The compliant element is placed along the cable transmission in order to compare its performance to the performance of actuators developed by other researchers. This compliant element would try and improve on the performance characteristics of these elements.

In order to provide these performance enhancements, several design requirements for the system were developed. The following high level design requirements needed to be addressed: provide exponential, stiffening characteristics to the compliant element; provide compliance along the cable; and, provide a good dynamic range.

In addition to these requirements, the compliant element should be compact in order to minimize the mass and volume placed on the cable. The element should be robust as to withstand unpredictable impact loads. It should be reliable, in order not to reduce the overall system reliability. Additionally, the compliant element should provide an accurate, stable and repeatable measure of force that the manipulator is experiencing.

3.3 Compliant Element Design

Based on the design requirements, several preliminary designs were developed and evaluated. One of the major constraints placed on the design of this device is the requirement that the compliant element be placed in line with the cable transmission. This constraint severely limited the space and weight allotted to the device. Furthermore, the placement of the element in line with the cable almost exclusively limited the compliant element motion to be in the axial direction. It was decided that a range of motion of approximately 0.5" would be sufficient to detect a large force range with the given instruments. Figure 3-1 shows the final design of the compliant element. Detailed design drawings for the device are shown in Appendix C. The overall dimensions of the compliant element are 2"x1.375"x1".

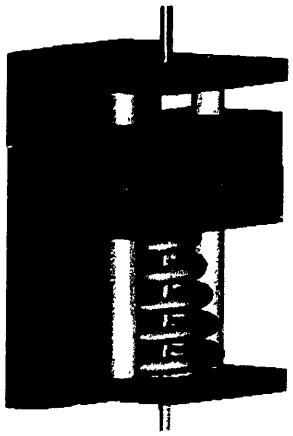

Figure 3-1: Final design of the compliant element

The design of the compliant element itself can be divided into a three major thrusts; selecting a suitable spring for the application, designing a housing for the spring that would ensure safe placement and convert the cable action in tension to spring compression, and providing low friction sliding motion to facilitate measurement of deflection.

The spring choice for the compliant element determines the force displacement characteristics for the element. Selecting a suitable spring provides a large dynamic range and good contact sensing capabilities. Choosing a suitable spring for this application presented us with tradeoff considerations from a space point of view and from a dynamic range point of view. Ideally, in order to allow for the smallest force to be detected, a very large diameter coil would be desired. This coil would provide a large deflection for a small applied force which would be easily detected. However, this large coil would require large space which would make the compliant element too bulky to place on the cable. Similarly, the number of turns and the smallest coil diameter determine the sensitivity of the element as it is subjected to higher loads. Several available 'off the shelf' springs were evaluated for their dynamic range and low force capability. A viable compromise between these design considerations was found to be the spring TA-2364 available from Century Spring Corp. which has its force displacement curve shown in Figure 2-3.

Once the appropriate spring for the application was selected, it was important that the spring be held in a safe and reliable manner in a housing. In addition, the housing would allow for cable tension to be transformed into spring compression. While the need for a sealed housing might be required for future applications as to provide protection from hazardous environments that might deteriorate performance, it was not deemed necessary for the prototype stage. The spring is held in the housing by being placed in a groove and being subjected to the preload force.

In addition to holding the spring safely, the housing should allow for a mechanism to provide a low friction measurement of deflection and as a result, a good, accurate

representation of the force across the spring. The lower the friction in the system, the better performance it could provide. A linear motion potentiometer is mounted on the back plate and is used for deflection measurement with the wiper attached to a sliding Delrin block. As the tension in the cable increases the Delrin block compresses the spring and changes the resistance of the potentiometer therefore providing a displacement measurement. In order to constrain the system, two parallel shafts were placed and the wiper was mounted on the Delrin block that would slide up and down the shafts. The main problem with this design was that the Delrin block would stick and slip on the shafts. In order to reduce the friction between the sliding Delrin block and the shafts. the Delrin block was fitted with ball bushings. As expected, the switch from sliding to rolling friction resulted in lower friction and improved performance of the compliant element.

3.4 Experimental Setup

To test the performance of the compliant element design, two separate experimental setups were used. The first test setup was unactuated and was used to obtain the force displacement characteristics for the compliant element. The second test setup was a one DOF prototype of the NSCA used to investigate its performance when subjected to some contact tests with different environments.

3.4.1 Compliant Element Characterization Setup

This test setup was used to obtain the force displacement curve for the compliant element. The compliant element was subjected to loads measuring from 1[g] to 5[kg]. The loads were in the form of weights hung from the cable in Figure 3-2 and a spring deflection measurement was obtained for each load.

In order to obtain these measurements, a Novotechnik, PTN-25 linear motion potentiometer and the S-115 wiper were used to obtain a spring deflection measurement. In order to provide low friction sliding motion between the Delrin block and the two

shafts, Thomson Industries Inc. Super 3 ball bushings were used. In order to obtain a detectable signal from the potentiometer, the output signal is amplified using the circuit shown in Appendix D.

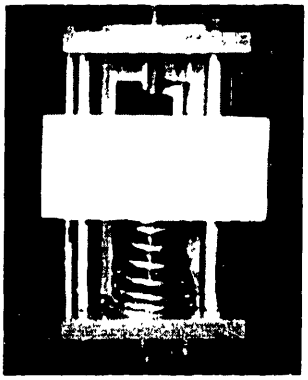

Figure 3-2: Force-displacement characterization setup

3.4.2 One DOF NSCA Test Setup

In order to verify the concept and test operation, a one DOF experimental test bed was constructed. This setup allows us to discover and correct any problems and issues with the current design prior to incorporating the NSCA design into the 4 DOF manipulator described in Chapter 4. The experimental setup is shown in Figure 3-3.

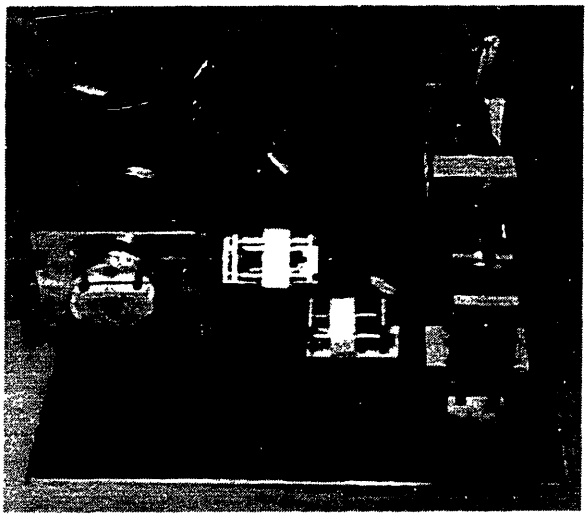

Figure 3-3: Nonlinear Series Compliance Actuator one DOF test setup

The motor used was a Maxon RE035 with a gearhead reduction of 36:1. Two compliant elements as described in the previous section were placed in line with the cable transmission. A Transducer Techniques TRT-50 torque sensor was used to verify results obtained. An HP5500-J06 encoder was placed on the output shaft as well to provide some insight into system dynamics. On the data acquisition side, a Sensable Technologies interface card was used to control the motor and obtain encoder readings while the analog signals from the compliant elements and the torque sensors were read using a National Instruments Lab-PC+ I/O card. The software for the system was a hybrid combination of Java and C. Low level control code was written in C and high level control and graphics were written in Java for simplicity.

3.5 Experimental Results

3.5.1 Force Displacement Curve for the Compliant Element

The use of compliant elements in line with a cable transmission requires an accurate knowledge of their force displacement characteristics in order to deduce the actual force or torque that the manipulator is applying. Figure 3-4 shows the force displacement curve for the compliant element and an exponential curve fit.

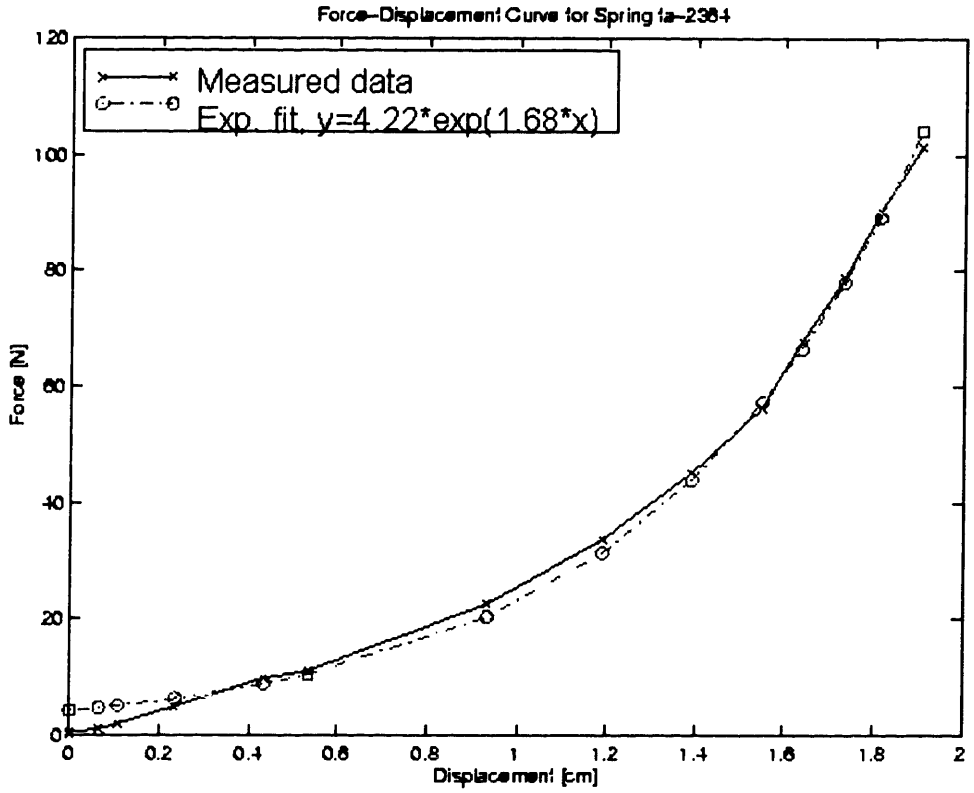

Figure 3-4: Force-displacement curve for TA-2364 spring, experimental results

It is interesting to note that the compliant element behaves as a constant stiffness spring up to the point where the first coil bottoms out. Beyond that point, the spring stiffens as is evident in the increasing slope of the curve. The smallest detectable force with this element was observed to be 0.098[N].

3.5.2 Position Control Performance

With the force-displacement curve for the compliant element available, the position control and force control capabilities of the one DOF test setup were investigated. This section will present the position control performance of the system as it is moving through free space. Based on the simulation results presented in Chapter 2 it was decided that the control scheme used on the system would be a simple PD controller.

The added phase from this controller makes the closed loop system more stable at low frequencies.

Using this controller the dynamic response of the closed loop system was evaluated. Sine waves varying in frequency were used as input to the system and the output response (encoder readings) was recorded. The frequency response of the system is shown in Figure 3-5. The resonant frequency of the system is 20[Hz] and the bandwidth of the system is around 25[Hz]. These plots are in agreement with the simulation results presented in section 2.6.

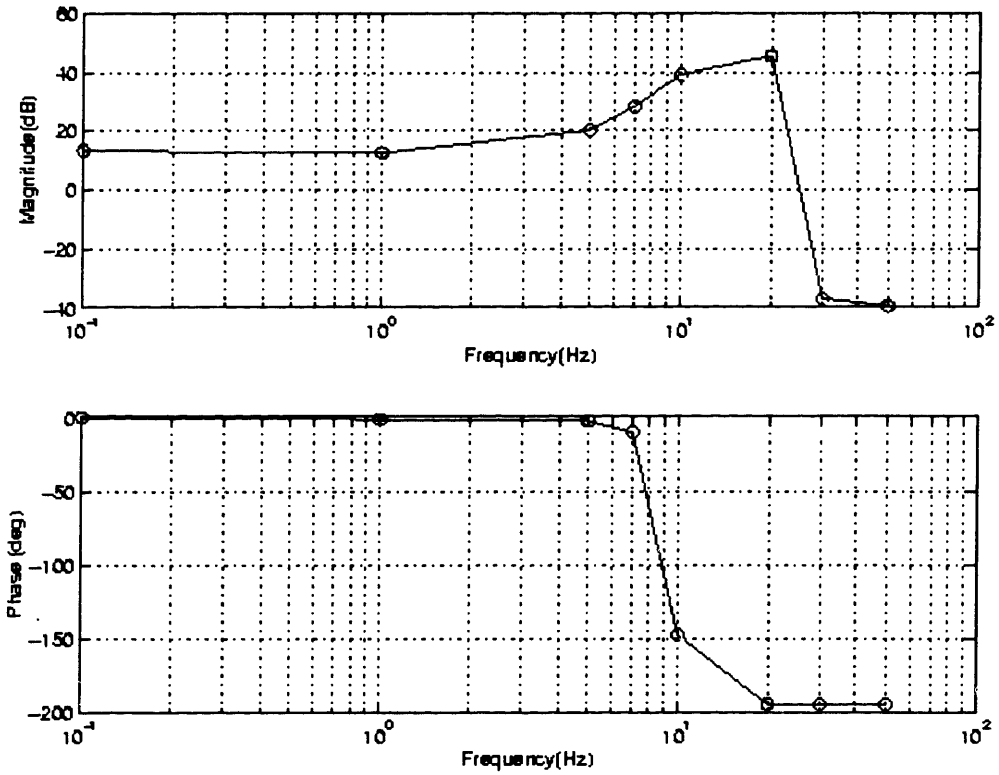

Figure 3-5: Frequency response of closed loop system, experimental results

3.5.3 NSCA Force Control Performance

Next, the performance of the system and its ability to apply forces or detect them while in contact with environments of different stiffness values is examined. A digging

manipulator is likely to encounter varied operating conditions such as different types of soil, buried obstacles (e.g. rocks) over a relatively small area. In order to operate in these unstructured environments in a safe, reliable and accurate way, the manipulator must be to establish initial contact in a controlled manner. The test case scenario was of the link travelling through free space and applying a specified force once contact is established. The controller tested out for this scenario expanded on the PD controller used for the movement through free space. In essence, position control was provided initially and the forces across the compliant elements were observed throughout the manipulator motion. If the forces reached a certain threshold it was determined that contact was established. At this point, a different control algorithm would become functional. This control algorithm implemented a proportional controller based on the forces experienced in the compliant elements. The derivative term for this controller was dropped because the signal proved too noisy to allow for derivative feedback.

Several experiments were conducted to fine tune the performance of the controller. Unfortunately, satisfactory performance was not achieved. The manipulator was able to establish contact and detect contact however, there were some difficulties in maintaining contact with the environment. I believe that this was most likely due to an error in the control code rather than a problem with the system.

3.5.4 Performance Parameters for Actuators

In addition to contact tests there are several other performance characteristics that are helpful for evaluating the performance of the system and the compliant element performance in particular. Again, due to lack of time these were not evaluated.

Some of the performance parameters, backdrive friction, peak steady state force and force resolution, are measured when the system is at steady state. The backdrive friction of the system measures the amount of force that is required to move the actuator when the system is not powered. The peak steady state force is of obvious importance to

the system. Force resolution is the smallest measurable force and is affected by sensor accuracy and noise and the quantization of the A/D conversion.

In order to provide a more complete picture of the system performance, dynamic performance characteristics require examination as well. These performance parameters include position response bandwidth (see Section 3.4.2) that is the frequency response of the system as it is moving through free space. Force control bandwidth is evaluated through the frequency response obtained when the end point for the system is fixed.

Other properties that are useful are the dynamic range of the system. One is the exertable dynamic range, that is the ratio between the largest and smallest force the manipulator can apply. Also, the dynamic range in sensing which relates the largest force the manipulator can detect to the smallest force it can detect.

Chapter 4 – Compliant Arm Design for Digging (CADD)

4.1 Motivation

The NSCA design discussed in the previous chapter is integrated into the arm design presented here. In conjunction with our sponsors, NASA/JPL, and in order to meet their goal of retrieving soil samples from Mars by the 2005-7 time frame we were required to design a digging manipulator. The manipulator would perform a variety of geological exploration tasks, most notably uncovering and acquiring soil samples from underneath the surface. In addition, the manipulator should be able to obtain mechanical soil properties such as hardness and cohesion. In order to perform this task successfully and in an efficient manner the manipulator should be able to apply and detect forces in an accurate manner over a large dynamic range.

Until recently, the WAM was used as a digging manipulator in our lab. The WAM was not designed for the purpose of rover based digging, yet it still managed to perform digging and trenching tasks quite well. However, it became apparent that performance enhancements in several areas could be achieved through the design of a new manipulator geared towards the task. One notable area for improvement was providing a kinematic configuration that would yield better maneuverability for digging and avoid points of singularity while performing the task. Another scope of improvements was the need for a more efficient, smaller scale manipulator that would more closely resemble an arm likely to be used in a mission scenario. Finally, there was a need for improved force sensing capabilities to allow for better manipulation through the application of accurate force and accurate sensing. As previously noted, the WAM is a backdrivable manipulator with very low backdrive friction. These system features allow reasonable force measurements to be obtained based on motor current sensing. However, confidence in these measurements was limited. The problem of sensing and applying reliable and accurate forces is even more inherent in the manipulator designs that are available at JPL. These manipulators have desirable kinematics but lack an accurate way

to measure forces. No force sensor is available and the significant gear reductions (on the order 1000:1) on the actuators make acquisition of accurate force data through motor current sensing very difficult.

Based on these system issues, it was decided that the new manipulator, the CADD, would maintain some desirable features of the WAM such as low friction cable drive transmission, and motor placement at the base. The CADD would also provide performance enhancements over the WAM in a few categories: provide a smaller, rover scale manipulator, provide a kinematic configuration better suited for digging, and improve force sensing capabilities using the idea of a compliant transmission.

4.2 Workspace Considerations

The first notable difference between the CADD and the WAM is the scale of the manipulator. The general goal was to try and have an arm could be rover mounted. Hence the scale of the rover played an important role in determining the dimensions of the arm. The scale of the FIDO rover designed for the 2003/5 mission currently stands at 1.176[m]x1.088[m]x0.51[m] (Lindemann, 1999). The working assumption was that the arm would be top mounted on the rover. This mounting location would provide better stability and the capability for applying larger forces than would be possible if the arm were mounted in a different location on the rover. The arm links were sized such that in its current mounting location, the manipulator would be able to reach all points on the ground around the rover.

4.3 Manipulator Kinematics

4.3.1 General Description

Based on the assigned workspace, work began to define the kinematics for the system. The kinematics for the manipulator were decided after conversations with fellow graduate students, Jesse Hong, Brian Anthony and Andrew Curtis. During a few meetings several possible kinematic configurations were suggested and evaluated for ease of manipulation and points of singularity. The kinematics selected for the CADD are similar to those of a backhoe (Figure 4-1a) with one added degree of freedom. The additional degree of freedom is the roll motion of the last link. Researchers (Hong, 1999b and Nathan, 1992) have shown that in order to reduce friction and avoid stick-slip behavior between the soil and the digging scoop or penetrating device it is helpful to introduce oscillations to the motion of the end effector. The roll motion could easily provide these desired oscillations as well as specify orientation for the end effector. A stick model of the kinematic configuration was constructed to qualitatively evaluate the design and find any points of singularity or other problem areas with the assigned kinematics and workspace. The general kinematic configuration of the manipulator can be seen in Figure 4-1b. The motions provided by the serial manipulator are yaw, pitch, pitch, and roll.

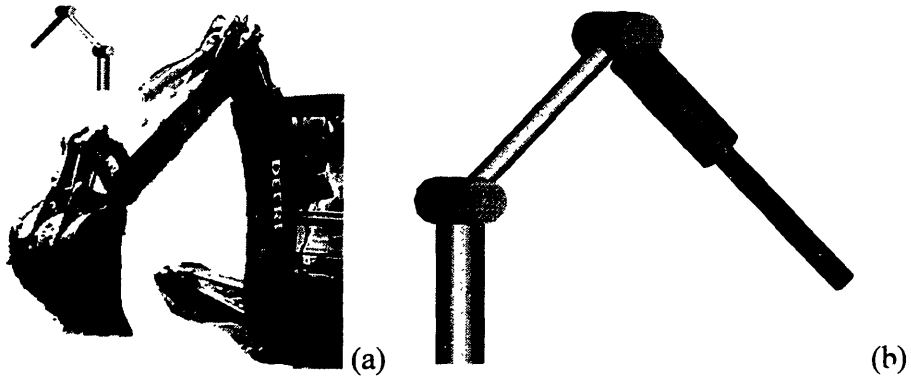

Figure 4-1: (a) A backhoe with its kinematic configuration, (b) Kinematics for CADD

4.3.2 Forward Kinematics

Given the general description of arm kinematics in the previous section, forward kinematics relating the joint variables to manipulator position and orientation were obtained. The manipulator link length and link offset parameters are presented in Table 4-1. Figure 4-2 relates those parameters to a sketch of the arm.

L_0	4.375"
L_1	13.25"
L_2	16"
D_2	1.375"

Table 4-1: Link parameters for the CADD

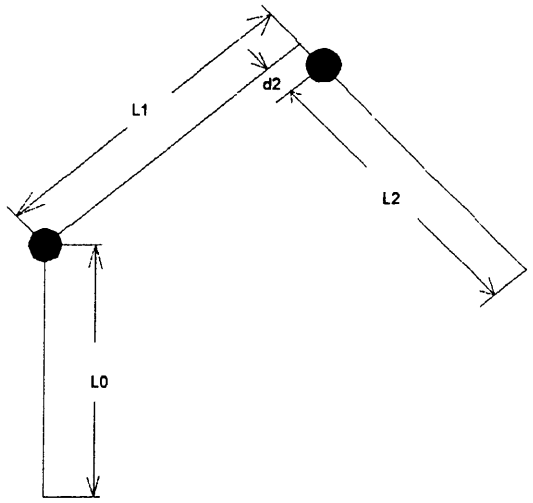

Figure 4-2: CADD link dimensions

Using the Denavit-Hartenberg (DH) notation (Craig, 1989), transformation matrices (see Appendix E) for the manipulator were generated and the forward kinematics for the manipulator obtained.

$$\begin{bmatrix} x \\ y \\ z \end{bmatrix} = \begin{bmatrix} -C\theta_1 S(\theta_2+\theta_3)l_2 + C\theta_1 C\theta_2 l_1 - C\theta_1 S\theta_2 d_2 - S\theta_1 l_0 \\ -S\theta_1 S(\theta_2+\theta_3)l_2 + S\theta_1 C\theta_2 l_1 - S\theta_1 S\theta_2 d_2 + C\theta_1 l_0 \\ -C(\theta_2+\theta_3)l_2 - S\theta_2 l_1 - C\theta_2 d_2 \end{bmatrix} \quad (4.1)$$

The position vector of the manipulator shows that the endpoint position is independent of the last degree of freedom which provides orientation for the end effector.

Another important characteristic for manipulators is the Jacobian matrix that can be used to find points of singularity and also transform motor joint torques to Cartesian forces.

$$J = \begin{bmatrix} S\theta_1 C(\theta_2+\theta_3)l_2 - S\theta_1 C\theta_2 l_1 + S\theta_1 S\theta_2 d_2 - C\theta_1 l_0 & -C\theta_1 C(\theta_2+\theta_3)l2 - C\theta_1 S\theta_2 l_1 - C\theta_1 C\theta_2 d_2 & -C\theta_1 C(\theta_2+\theta_3)l_2 & 0 \\ -C\theta_1 S(\theta_2+\theta_3)l_2 + C\theta_1 C\theta_2 l_1 - C\theta_1 S\theta_2 d_2 - S\theta_2 l_0 & -S\theta_1 C(\theta_2+\theta_3)l_2 - S\theta_1 S\theta_2 l_1 - S\theta_1 C\theta_2 d_2 & -S\theta_1 C(\theta_2+\theta_3)l_2 & 0 \\ 0 & S(\theta_2+\theta_3)l_2 - C\theta_2 l_1 + S\theta_2 d_2 & S(\theta_2+\theta_3)l_2 & 0 \end{bmatrix} \tag{4.2}$$

As expected, the Jacobian matrix for the manipulator shows independence from the last degree of freedom. Points of singularity for the system exist on the workspace boundaries and also when the end point is aligned with the axis of rotation of the first degree of freedom as shown in Figure 4-3.

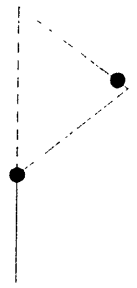

Figure 4-3: Singular configuration of the CADD

It is important to note that this singular configuration should not interfere with the task performance of the manipulator. This singular configuration as is corresponds to the manipulator operating in free space above ground which is unlikely for the digging task. Similarly, the mirror image of this configuration has the manipulator trying to dig underneath the rover which is also an unlikely scenario.

4.4 Actuator Selection

In order to provide the proper output forces required for the digging, suitable actuators must be selected. Two methods were used to evaluate the forces that are required for the digging task. One source of obtaining force data for the task was experiments conducted by Hong (Hong, 1999a) using the WAM system and backing out force information using motor current sensing. A second source of force data was obtained via the unactuated wooden mock up shown in Figure 4-4. The wooden mock up was assembled in collaboration with Andrew Curtis and the forces required for digging were observed using a spring scale for different strokes through different soils. The force measurements obtained from both sources were in agreement and found that the planar forces required for digging were on the order of 5[lbs].

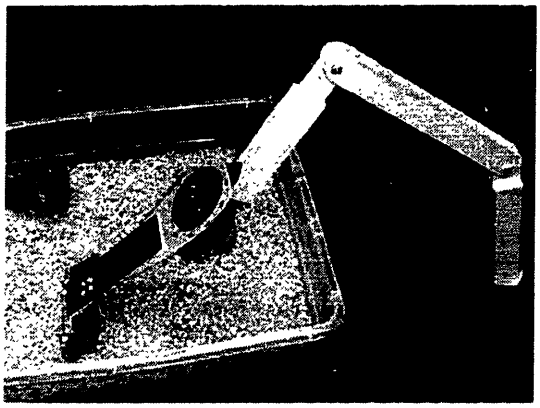

Figure 4-4: Force measurement setup

Based on the experimentally obtained force values for digging and on the proposed link lengths, the torque required at the motor was calculated assuming a worst case scenario of only one motor to provide the force. A torque of 16.4[Nm] was required at the motor to produce the desired 5[lbs.] force at the endpoint. Several motor and gearhead assemblies were evaluated for their torque output and power to weight ratio. The Maxon RE series motors were selected due to their good power to weight ratio and their availability. One of the limiting factors in choosing a motor-gearhead assembly was the maximum torque rating of the gearhead. Some smaller motors with larger reductions

could provide the same output torque, however, the actual torque output was limited due to the shear strength of the gearhead teeth which might break under a backdrive torque. The motors selected were the Maxon RE035 with a 72:1 gearhead capable of providing a maximum torque of 77[Nm], providing a safety factor of 4.7.

4.6 Mechanical Design

Transforming the kinematic parameters and workspace requirements into a physical manipulator presented many interesting design challenges. The design task of the CADD was undertaken in collaboration with Andrew Curtis. The greatest design challenges were presented as a result of our desire to introduce compliant transmission as method for improving the dynamic range of forces applied and of forces sensed. Figure 4-5 shows the CADD assembly without the cable transmission and electronic circuitry.

Two different compliant transmission ideas were implemented in the manipulator. The concept presented in this work of providing compliance in line with the cable transmission is integrated into the last two degrees of freedom (pitch and roll, controlled by motors 3 and 4 in Figure 4-5) of the manipulator. The compliant transmission element designed by Curtis (Curtis, 1999) in the form of a nonlinear compliant coupling acting in torsion is incorporated into the first two degrees of freedom (yaw and pitch, controlled by motors 1 and 2 respectively in Figure 4-5) of the system.

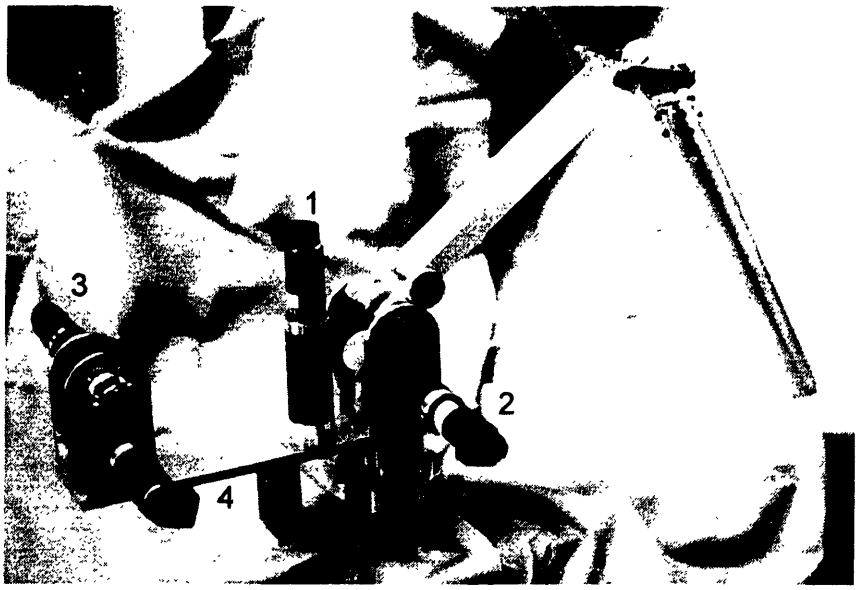

Figure 4-5: The CADD assembly

The decision of which compliant transmission concept to implement on which degree of freedom was mainly based on evaluating the ease of integration into the system of each compliant element for every degree of freedom. The NSCA presented in this thesis yields itself best to placement in line with the cable transmission (as shown in section 3.4.2) and as a result needs to have part of the cable circuit to travel on. The design developed by Curtis is a coupling that can be mounted onto the motor shaft or one that can be mounted to the output shaft. Due to the size of this compliant element, it was better suited for the larger joints closer to the base of the manipulator.

Based on the compliant element designs, it was decided that the actuator design presented in this work is best suited for use in the last two degrees of freedom of the manipulator. Given the weight and size of the motors and drawing on the WAM design, the motors are placed close to the base of the manipulator and power is transmitted to the joints via cables. The long cable paths between the motors and the last two degrees of freedom are ideal locations for placing the compliant elements on the cable. It is vital that space is budgeted to allow for unobstructed movement of the compliant elements along the cable circuit as full range of motion for the joint might not be achieved otherwise.

Figure 4-6 shows a CAD model displaying the compliant elements location along the cable transmission system.

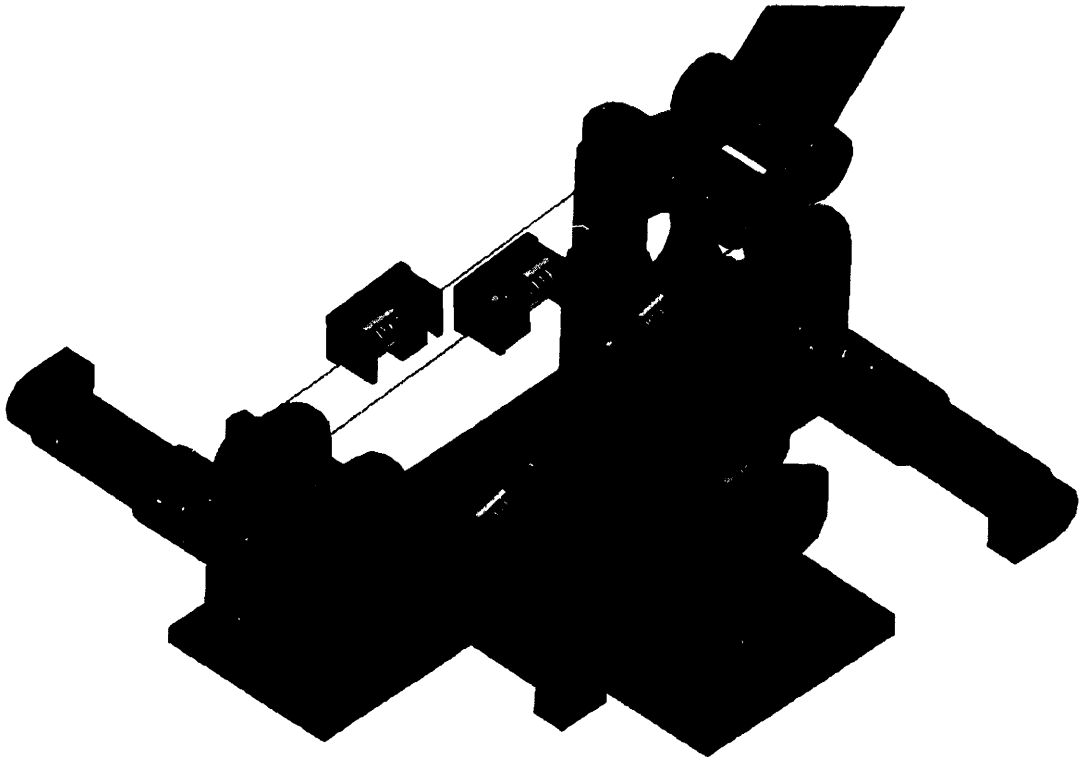

Figure 4-6: Compliant element location on the cable circuit

The 2 DOF cable driven differential using the compliant actuator developed in this work is shown in Figure 4-7, controlled by motors 3 and 4 (see Figure 4-5) and is used to provide the last two degrees of freedom for the system. Detailed CAD drawings are shown in Appendix F. The differential was chosen since it allows for a compact 2 DOF assembly and mates well with the compliant element design by allowing for the motors to be placed on the base link. There are two major separate cable assemblies for the system. The first assembly that consists of two cable circuits connects the each side of the differential to its respective motor. The second assembly couples the two sides of the differential to provide the pitch and roll motion required.

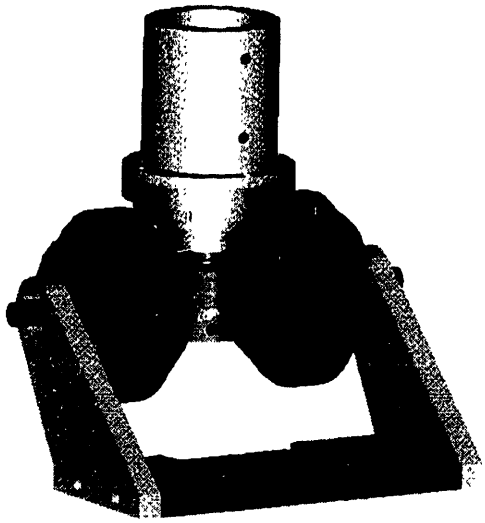

(a)

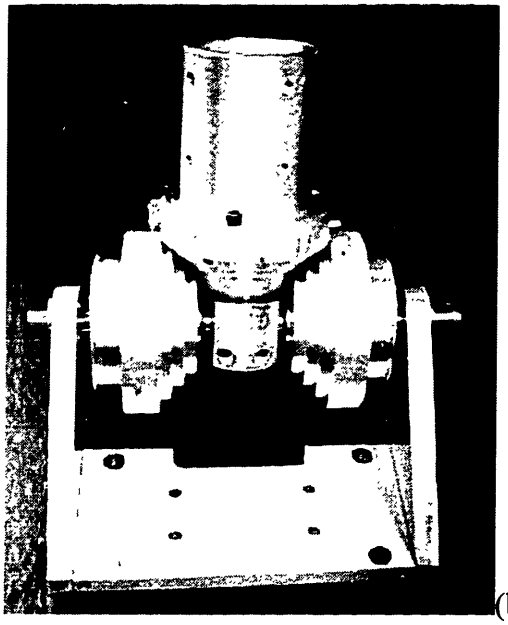

(b)

Figure 4-7:(a) CAD rendition of differential design, (b) Assembled differential

Chapter 5 – Conclusions

5.1 Review of Thesis

In conclusion, this work presented the design of a nonlinear series compliance actuator for use in cable driven transmissions. The actuator provides nonlinear compliance via a compliant element placed in line with a cable transmission. Performance characteristics of this element were evaluated. Experiments performed to evaluate the actuator's performance show an exponential force displacement curve as predicted. Additional experiments determined he position control bandwidth of the system to be 25[Hz]. A 4 DOF robotic digging manipulator was designed in collaboration with Andrew Curtis. The nonlinear compliance actuator presented in this work is integrated into the system to control 2 DOFs of the arm.

5.2 Further Work

The suggested areas for further work fall into three major categories: finishing up characterizing the actuator performance, improvements to the actuator itself, and utilizing the CADD.

In Chapter 3, metrics of interest in evaluating actuator performance are discussed. Those metrics should be revisited so that a more complete model of the actuator performance can be obtained.

The mechanical design of the actuator is another area where improvements could be provided. A method for allowing a quick change of the spring used in the compliant element would prove useful. Additionally, the option of altogether locking out the compliance 'on the fly' would allow the actuator to perform well in tasks requiring contact with the environment and tasks where a stiff manipulator is required. Another

interesting area to study is the application of preload tension to the cable transmission system without sacrificing losing sensitivity of the compliant element.

Finally, utilizing the CADD for digging tasks would provide us with a way of comparing the performance of this manipulator to the performance of traditional stiff transmission manipulators.

Bibliography

Ananthasuresh, G.K. and Kota, S. (1995). Designing compliant mechanisms. *Mechanical Engineering*, 117(11):93-96.

Childs, P.R.N. (1998). *Mechanical Design.* John Wiley and Sons.

Craig, J.J. (1989). *Introduction to Robotics Mechanics and Control.* Addison-Wesley.

Curtis, A.W. (1999). Personal Communication.

Erickson, W.D. (1987). *Belt Selection and Application for Engineers.* Marcel Dekker.

Hogan, N. (1985). Impedance control: An approach to manipulation: Part 1 – theory, Part 2 – implementation, Part 3 – applications. *ASME Journal of Dynamic Systems, Measurement and Control*, 107:1-24.

Hong, W.J. (1999a). Personal Communication.

Hong, W.J. and Salisbury, J.K. (1999b). Obstacle negotiation in robotic excavation. Submitted to the *IASTED Robotics and Applications 1999 Conference.*

Iberall, T. (1997). Human prehension and dexterous robot hands. *The International Journal of Robotics Research*, 16(3):285-299.

Lindemann, R. <ralinde @mail1.jpl.nasa.gov> "Re: some questions from Salisbury's group at MIT." 29 January 1999. Personal e-mail.

Madhani, A.J. (1998). Design of teleoperated surgical instruments for minimally invasive surgery. Ph.D. Thesis, MIT Department of Mechanical Engineering.

Michelman ,P. and Allen, P. (1993). Compliant manipulation with a dexterous robot hand. In *Proceedings of the IEEE International Conference on Robotics and Automation*, volume 3, pp. 711-6, Atlanta, GA.

Morrell, J.B. (1996). Parallel Coupled Micro-Macro Actuators. Ph.D. Thesis, MIT Department of Mechanical Engineering.

Nagai, K. et al. (1997). Development of a redundant macro-micro manipulator for compliant motion. In Proceedings of the 1997 8th International Conference on Advanced Robotics (ICAR-97), pp.707-12, Monterey, CA.

Nathan, M. et al. (1992). A comparison of the lunar efficiencies of a new class of lunar excavation tools. *Space Exploration Science and Technologies Research*, 31:141-151.

Pelletier, M. and Daneshmend, L.K. (1997). Automatic synthesis of robot compliant motions in dynamic environments. International Journal of Robotics Research, 16(6):730-748.

Pratt, G.A. and Williamson, M.W. (1995a). Series elastic actuators. In *Proceedings of the IEEE/RSJ International Conference on Intelligent Robots and Systems (IROS-95)*, volume 1, pp. 399-406, Pittsburgh, PA.

Pratt, G.A. et al. (1995b). Stiffness isn't everything. In *Proceedings of the Fourth International Symposium on Experimental Robotics (ISER-95)*, Stanford, CA.

Pratt, J. (1996). Effects of spring constant on series elastic actuator stability, dynamic range, and large force bandwidth. Unpublished work.

Raibert, M.H and Craig, J.J. (1981). Hybrid position/force control of manipulators. *Journal of Dynamic Systems, Measurement and Control*, 102:126-133.

Salisbury, K. et al (1988). Preliminary Design of a whole-arm manipulation system(WAMS). *Proceedings of the 1988 IEEE International Conference on Robotics and Automation*, pp. 254-260. Philadelphia, PA.

Sawada, C. (1995). Evaluating the performance of robotic compliant tasks according to power consumption: approach and applications. In *Proceedings of the IEEE International Conference on Robotics and Automation*, volume 1, pp. 1146-53, Nagoya, Japan.

Shah, V.K. (1997). Design and control of a nonlinearly compliant robotic finger. M.S. Thesis, MIT Department of Mechanical Engineering.

Srinivasan, M. and Chen, J.(1993). Human performance in controlling normal forces of contact with rigid objects. *ASME Dynamic Systems and Control: Advances in Robotics, Mechatronics, and Haptic Interfaces*, DSC-49.

Sugano, S., Tsuto, S., Kato, I. (1992). Force control of the robot finger joint equipped with mechanical compliance adjuster. In *Proceedings of the IEEE/RSJ International Conference on Intelligent Robots and Systems*, pp. 2005-13.

Wahl, A.M. (1963). *Mechanical Springs*. McGraw-Hill.

Whitney, D.E. (1982). Quasi-static assembly of compliantly supported rigid parts. *Journal of Dynamic Systems, Measurement and Control*, 104:65-77.

Williamson, M.W. (1995). Series elastic actuator. M.S. Thesis, MIT Department of Electrical Engineering and Computer Science.

Williamson, M.W. (1999). Robot Arm Control Exploiting Natural Dynamics. Ph.D. Thesis, MIT Department of Electrical Engineering and Computer Science.

Appendix A – Matlab Simulation of Force Displacement Curves

```
% program to approximate stiffening behaviour of conical compression
springs
%each coil is a spring w/ const. stiffness, and the next coil is active
once
%the previous coil bottomed out

close all; %clears out all graphic windows
clear all;

%input starting diameter, ending diameter, wire diameter, height
%and number of turns

%springnum=input('Enter spring catalog number: ');
%outd=input('Enter outside diameter: ');
%ind=input('Enter inside diameter: ');
%wired=input('Enter wire diameter: ');
%height=input('Enter spring height: ');
%coils=input('Enter # of active coils: ');

%data for all springs to be analyzed
dataspring=[2091 0.421   0.343   0.81    0.047   6;...
2137 0.296   0.219   0.41    0.046   8;...
2093 0.328   0.234   1.25    0.04    9;...
2364 0.609   0.297   1       0.051   8;...
2204 0.328   0.203   0.72    0.04    10;...
2234 0.5     0.343   1       0.059   8;...
2200 0.625   0.328   2       0.057   10;...
2318 0.625   0.375   0.38    0.029   4];

for numspri=1:length(dataspring)


%block to make testing easier
springnum=dataspring(numspri,1);
outd=dataspring(numspri,2);
ind=dataspring(numspri,3);
height=dataspring(numspri,4);
wired=dataspring(numspri,5);
coils=dataspring(numspri,6);


%calculate the spring rate

%parameters:
% K=spring rate (lbs/in.)
% G=modulus (spring steel 11.5e6, stainless=10e6)
% d=wire diameter (in.)
% n=number of active coils (one in this case)
% D=mean diameter (O.D.-d) inches


G=11.5e6; %assume mat'l is stainless steel
```

```
d=wired;
n=coils;
D=outd-wired;

%K=G*d^4/(8*n*D^3);

%find pitch
pitch=(height-coils*wired)/coils;

%there are as many spring constants as there are active coils each one
of
%them is effective only when the previous spring bottoms out and until
that
%spring itself bottoms out

rbig=outd/2;
rsmall=ind/2;
%define the various springs
for g=0:1:coils
      r=rbig-(g*(pitch+wired)*((rbig-rsmall)/height));
      dia=2*r;
      k(g+1)=G*d^4/(8*n*dia^3);
end

count=0;
oldsel=0;
maxdefl=coils*pitch;
xold=0;
oldforce=0;
totforce=0;
delta=0.001;

for xx=0:delta:maxdefl
      count=count+1;
      disp(count)=xx;
      newsel=floor(xx/pitch);
      %check to see if spring bottomed out
      totforce=totforce+delta*k(newsel+1);
      force(count)=totforce;
end


%X0=[1 1 1]';

X0=[1 1]';

x=leastsq('fit_simp', X0, [], [], disp, force);

%Y_new=x(1)+x(2).*exp(x(3).*disp);

Y_new=x(1).*exp(x(2).*disp);
figure
plot(disp,force,'b', disp, Y_new,'-.r');
%plot(disp,force);

xlabel('displacement (in)');
ylabel('force (lbs)');
```

```
title(['Force displacement curve for ta-',num2str(springnum)]);

%gtext(['y=',num2str(x(1)),'+',num2str(x(2)),'*exp(',num2str(x(3)),'*x)
']);
gtext(['y=',num2str(x(1)),'*exp(',num2str(x(2)),'*x)']);

print -dbmp256 temp;
clear disp force Y_new

end
```

Appendix B – Simulink model of dynamic system

The following simulink model was used to evaluate the dynamic performance of the nonlinear system.

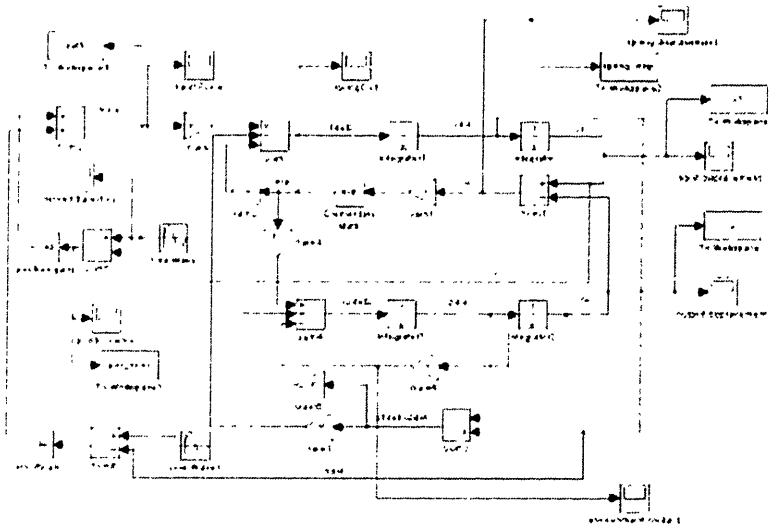

The following file was used to initiate the parameters for the simulation.

```
%initialize the simulink file
clear all;
m1=50; %mass1
m2=0.1*m1; %mass2
c=0.28041; %spring parameter
a=306.9542; %spring parameter
%c=4.81;  %spring parameter
%a=0.52;  %spring parameter

%f1=1; %force
b=50; %damping term
k0=0; %environment stiffness

kp=1000; %position gain
kv=0.05; %velocity gain
ki=5;

%for the input sine wave
freq=2;
ww=2*pi*freq;
ampli=100;
```

Appendix C – CAD Drawings for the Compliant Element Design

Part	Quantity
Bottom Cap	1
Top Cap	1
New Pot Hold	1
Wiper Holder	1
Slider	2

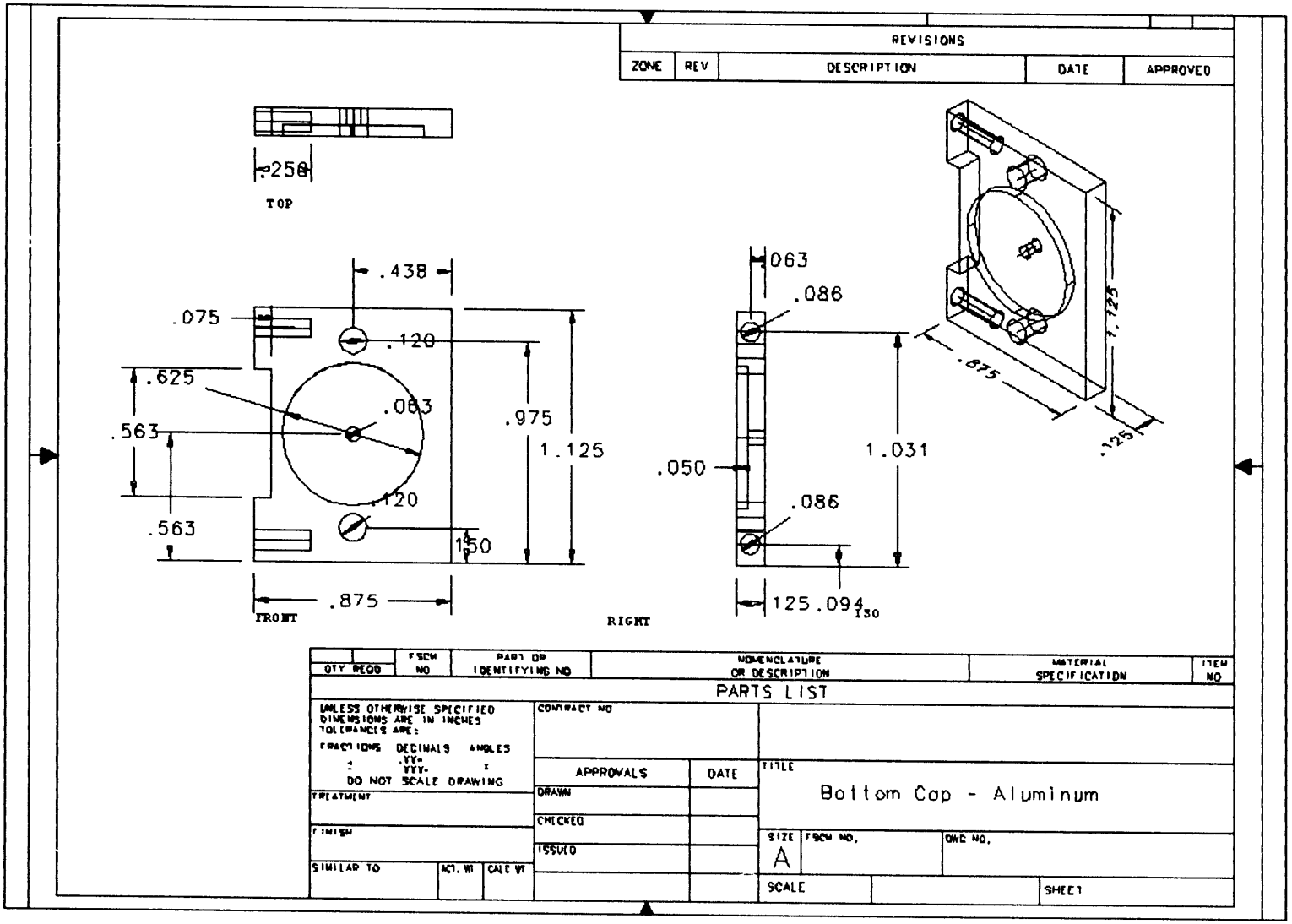
REVISIONS
ZONE
REV
DESCRIPTION
DATE
APPROVED
.250
TOP
.438
.075
.120
.625
.083
.563
.975
1.125
.120
.563
.150
.875
FRONT
.063
.086
.050
1.031
.086
.125
.094
ISO
RIGHT
1.125
.875
.125
QTY REQD
FSCM NO
PART OR IDENTIFYING NO
NOMENCLATURE OR DESCRIPTION
MATERIAL SPECIFICATION
ITEM NO
PARTS LIST
UNLESS OTHERWISE SPECIFIED
DIMENSIONS ARE IN INCHES
TOLERANCES ARE:
FRACTIONS
DECIMALS
.XX=
.XXX=
ANGLES
DO NOT SCALE DRAWING
CONTRACT NO
APPROVALS
DATE
DRAWN
CHECKED
ISSUED
TREATMENT
FINISH
SIMILAR TO
MAT'L
CALC WT
TITLE
Bottom Cap - Aluminum
SIZE
A
FSCM NO.
DWG NO.
SCALE
SHEET

REVISIONS				
ZONE	REV	DESCRIPTION	DATE	APPROVED

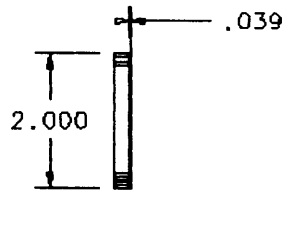

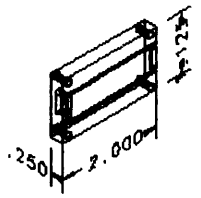

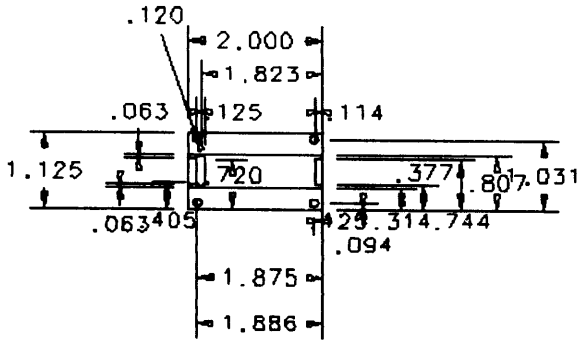

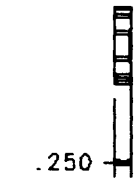

FRONT

TOP

QTY REQD	FSCM NO	PART OR IDENTIFYING NO	NOMENCLATURE OR DESCRIPTION	MATERIAL SPECIFICATION	ITEM NO
PARTS LIST					

UNLESS OTHERWISE SPECIFIED
DIMENSIONS ARE IN INCHES
TOLERANCES ARE:
FRACTIONS DECIMALS ANGLES
± .XX± ±
.XXX±
DO NOT SCALE DRAWING

TREATMENT

FINISH

SIMILAR TO | MAT. SP | CAGE NO

CONTRACT NO

APPROVALS	DATE
DRAWN WRIGHT	
CHECKED ISO	
ISSUED	

TITLE
New Pot Hold - Aluminum

SIZE A | FSCM NO. | DWG NO.

SCALE | SHEET

REVISIONS				
ZONE	REV	DESCRIPTION	DATE	APPROVED

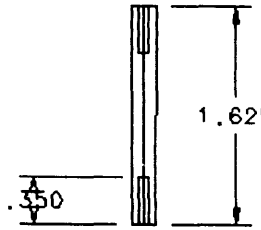

TOP

ISO

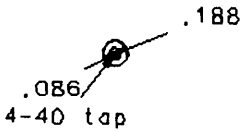

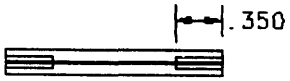

FRONT

RIGHT

QTY REQD	FSCM NO	PART OR IDENTIFYING NO	NOMENCLATURE OR DESCRIPTION	MATERIAL SPECIFICATION	ITEM NO

PARTS LIST

UNLESS OTHERWISE SPECIFIED
DIMENSIONS ARE IN INCHES
TOLERANCES ARE:
FRACTIONS ± DECIMALS .YY= .YYY= ANGLES ±
DO NOT SCALE DRAWING

CONTRACT NO

APPROVALS	DATE
DRAWN	
CHECKED	
ISSUED	

TREATMENT

FINISH

SIMILAR TO | ACT. WT | CALC WT

TITLE: Slider - Stainless Steel

SIZE A | FSCM NO. | DWG NO.

SCALE | SHEET

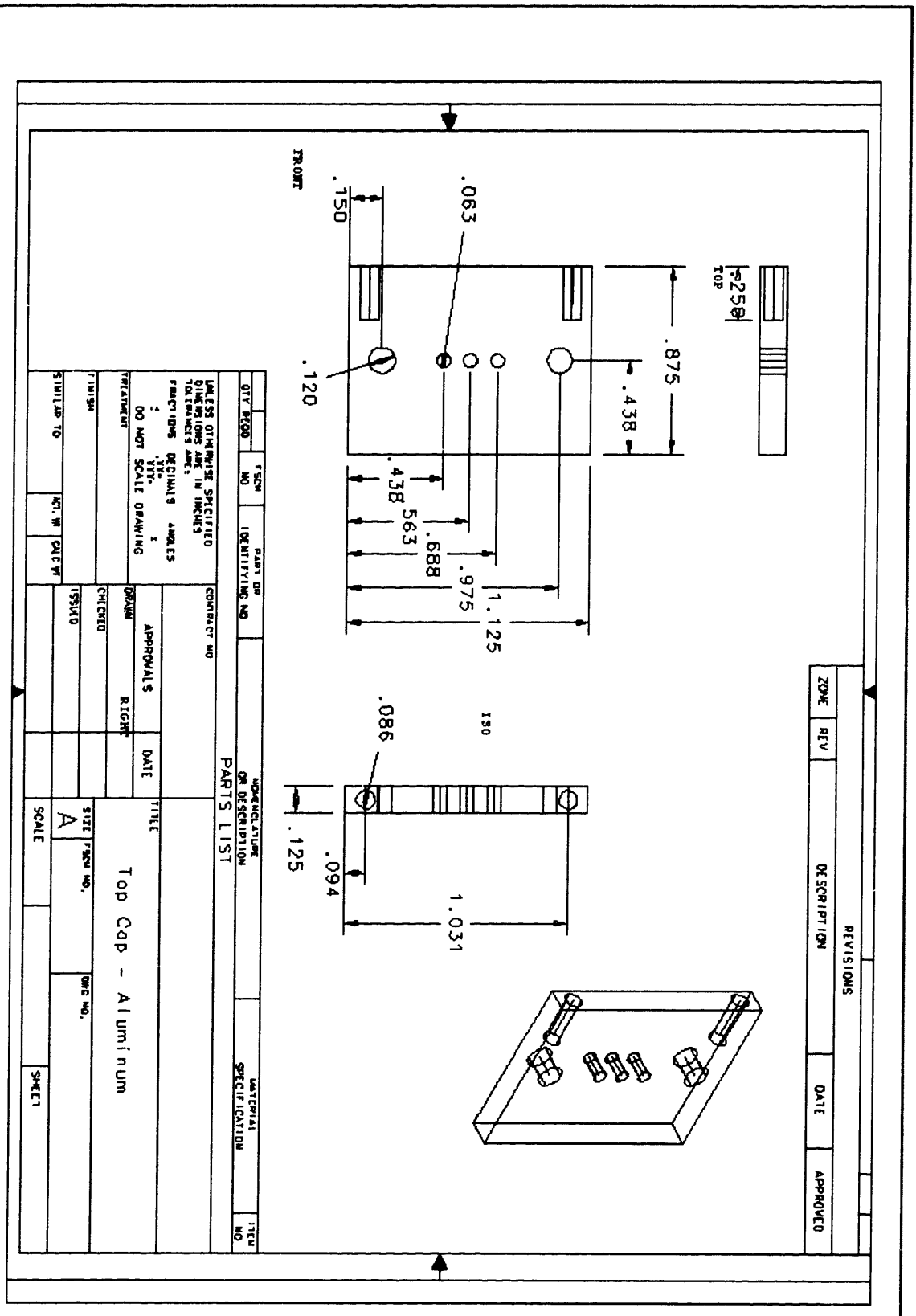
REVISIONS
ZONE
REV
DESCRIPTION
DATE
APPROVED
.250
TOP
.875
.438
.063
.150
.120
FRONT
.438
.563
.688
.975
1.125
ISO
.086
.125
.094
1.031
PARTS LIST
Top Cap - Aluminum

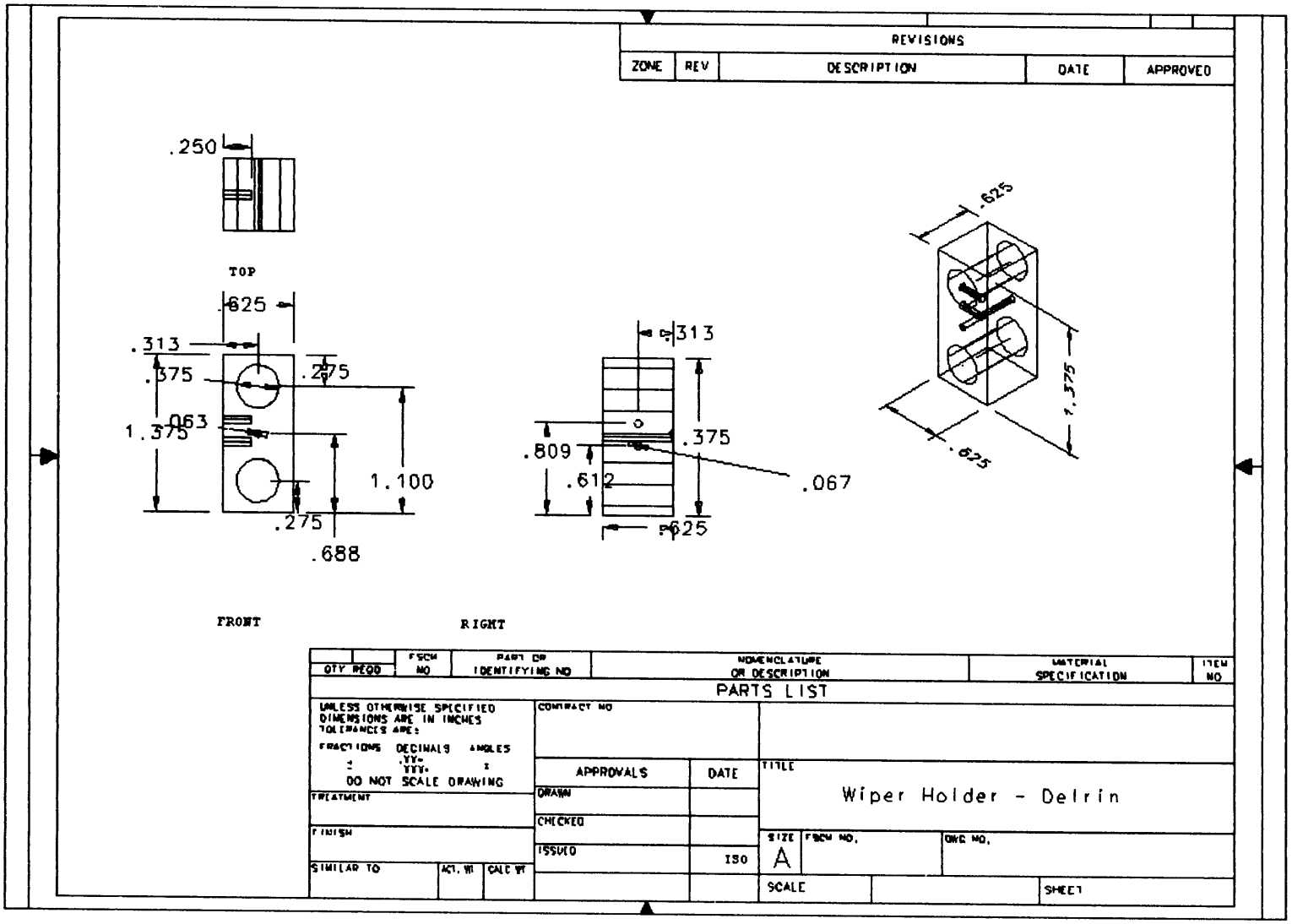
REVISIONS
ZONE
REV
DESCRIPTION
DATE
APPROVED
.250
TOP
.625
.313
.375
.275
.063
1.375
1.100
.275
.688
FRONT
.313
.375
.809
.612
.067
.625
RIGHT
.625
1.375
.625
QTY REQD
FSCM NO
PART OR IDENTIFYING NO
NOMENCLATURE OR DESCRIPTION
MATERIAL SPECIFICATION
ITEM NO
PARTS LIST
UNLESS OTHERWISE SPECIFIED DIMENSIONS ARE IN INCHES
TOLERANCES ARE:
FRACTIONS
DECIMALS .YY= .YYY=
ANGLES ±
DO NOT SCALE DRAWING
CONTRACT NO
APPROVALS
DATE
DRAWN
CHECKED
ISSUED
ISO
TREATMENT
FINISH
SIMILAR TO
MAT'L
CAGE NO
TITLE
Wiper Holder - Delrin
SIZE
A
FSCM NO.
DWG NO.
SCALE
SHEET

Appendix D – Amplifier Circuit for Compliant Element Signal

Due to the severe current limitation on the linear motion potentiometer, the following amplifier circuit (Shah, 1997) was built to provide a useable range of signals.

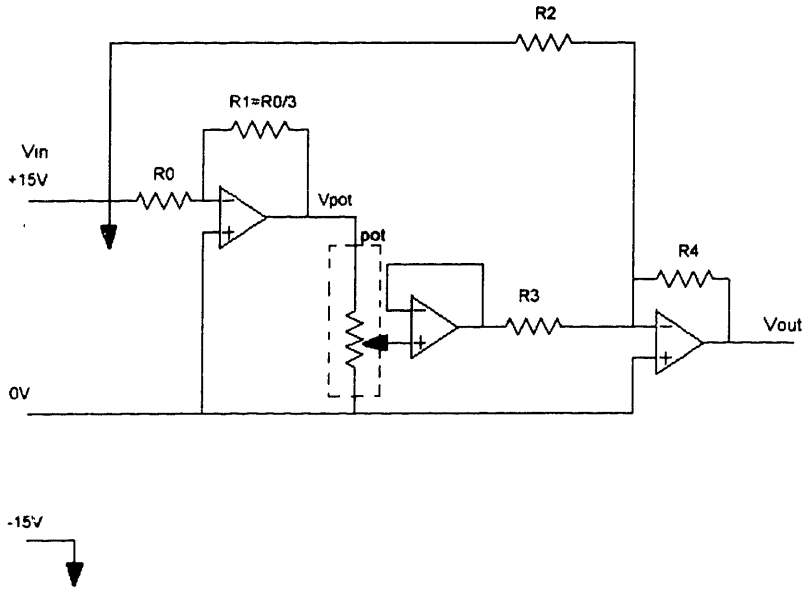

The output of the circuit is given by the following equation:

$$V_{out} = -\frac{R_4}{R_2}V_{in} - \frac{R_4}{R_3}V_{pot}$$

The following components were used in the circuit. The operational amplifiers were National Semiconductor LF347BN.

Resistor values are shown in the following table:

R_0	15kΩ
R_1	5kΩ
R_2	15kΩ
R_3	2.5kΩ
R_4	5kΩ

Appendix E – transformation matrices

The following figure shows the frame assignments for the manipulator.

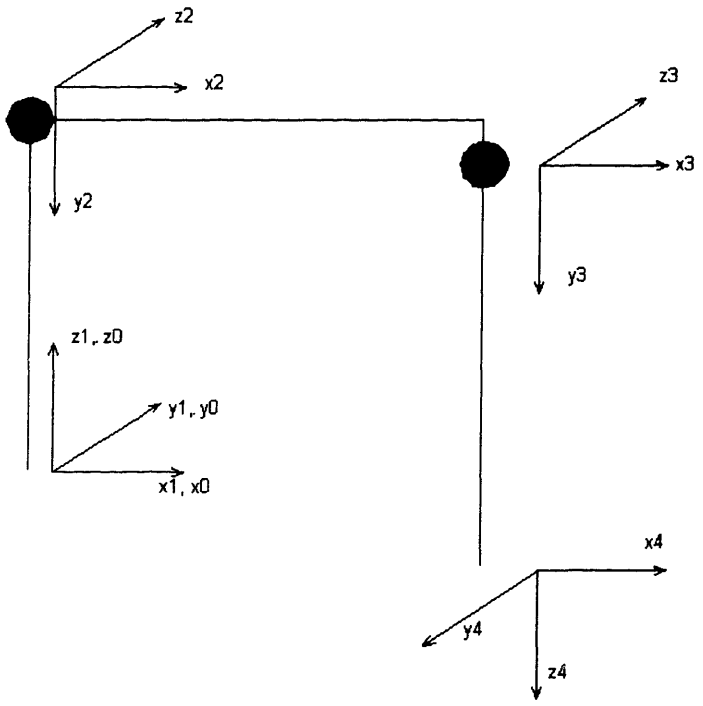

The following transformation matrices can be written based on the frame assignments.

$$A_{01} = \begin{bmatrix} \cos\theta_1 & -\sin\theta_1 & 0 & 0 \\ \sin\theta_1 & \cos\theta_1 & 0 & 0 \\ 0 & 0 & 1 & 0 \\ 0 & 0 & 0 & 1 \end{bmatrix}$$, representing the first degree of freedom, yaw.

$$A_{12} = \begin{bmatrix} \cos\theta_2 & -\sin\theta_2 & 0 & 0 \\ 0 & 0 & 1 & l_0 \\ -\sin\theta_2 & -\cos\theta_2 & 0 & 0 \\ 0 & 0 & 0 & 1 \end{bmatrix}$$, representing the second degree of freedom, pitch.

$$T_{23} = \begin{bmatrix} 1 & 0 & 0 & l_1 \\ 0 & 1 & 0 & d_2 \\ 0 & 0 & 1 & 0 \\ 0 & 0 & 0 & 1 \end{bmatrix}$$, moves the reference frame to the base of the differential.

$$A_{23} = \begin{bmatrix} \cos\theta_3 & -\sin\theta_3 & 0 & 0 \\ \sin\theta_3 & \cos\theta_3 & 0 & 0 \\ 0 & 0 & 1 & 0 \\ 0 & 0 & 0 & 1 \end{bmatrix}$$, represents the third degree of freedom, differential pitch.

$$A_{34} = \begin{bmatrix} \cos\theta_4 & -\sin\theta_4 & 0 & 0 \\ 0 & 0 & 1 & l_2 \\ -\sin\theta_4 & -\cos\theta_4 & 0 & 0 \\ 0 & 0 & 0 & 1 \end{bmatrix}$$, represents the fourth degree of freedom, differential roll.

And, the transformation from the base to endpoint is represented by:

$$T_{05} = A_{01} * A_{12} * T_{23} * A_{23} * A_{34}$$

$$T05 = \begin{bmatrix} C\theta_1 C\theta_{23} C\theta_4 + S\theta_1 S\theta_4 & -C\theta_1 C\theta_{23} S\theta_4 - S\theta_1 C\theta_4 & -C\theta_1 S\theta_{23} & -C\theta_1 S\theta_{23} l_2 + C\theta_1 C\theta_2 l_1 - C\theta_1 S\theta_2 d_2 - S_1 l_0 \\ S\theta_1 C\theta_{23} C\theta_4 - C\theta_1 S\theta_4 & -S\theta_1 C\theta_{23} S\theta_4 - C\theta_1 C\theta_4 & -S\theta_1 S\theta_{23} & -S\theta_1 S\theta_{23} l_2 + S\theta_1 C\theta_2 l_1 - S\theta_1 S\theta_2 d_2 + C_1 l_0 \\ -S\theta_{23} C\theta_4 & S\theta_{23} S\theta_4 & -C\theta_{23} & -C\theta_{23} l_2 - S\theta_2 l_1 - C\theta_2 d_2 \\ 0 & 0 & 0 & 1 \end{bmatrix}$$

Appendix F – CAD Drawings for differential design

Part	Quantity
Base Plate	1
Differential1	1
Differential2	1
Extension Drum	2
Link3 tube	1
Pitch	1
PR holder	2
Roll	1
Shaft	1
Tension Block	2
Tube Connect	1

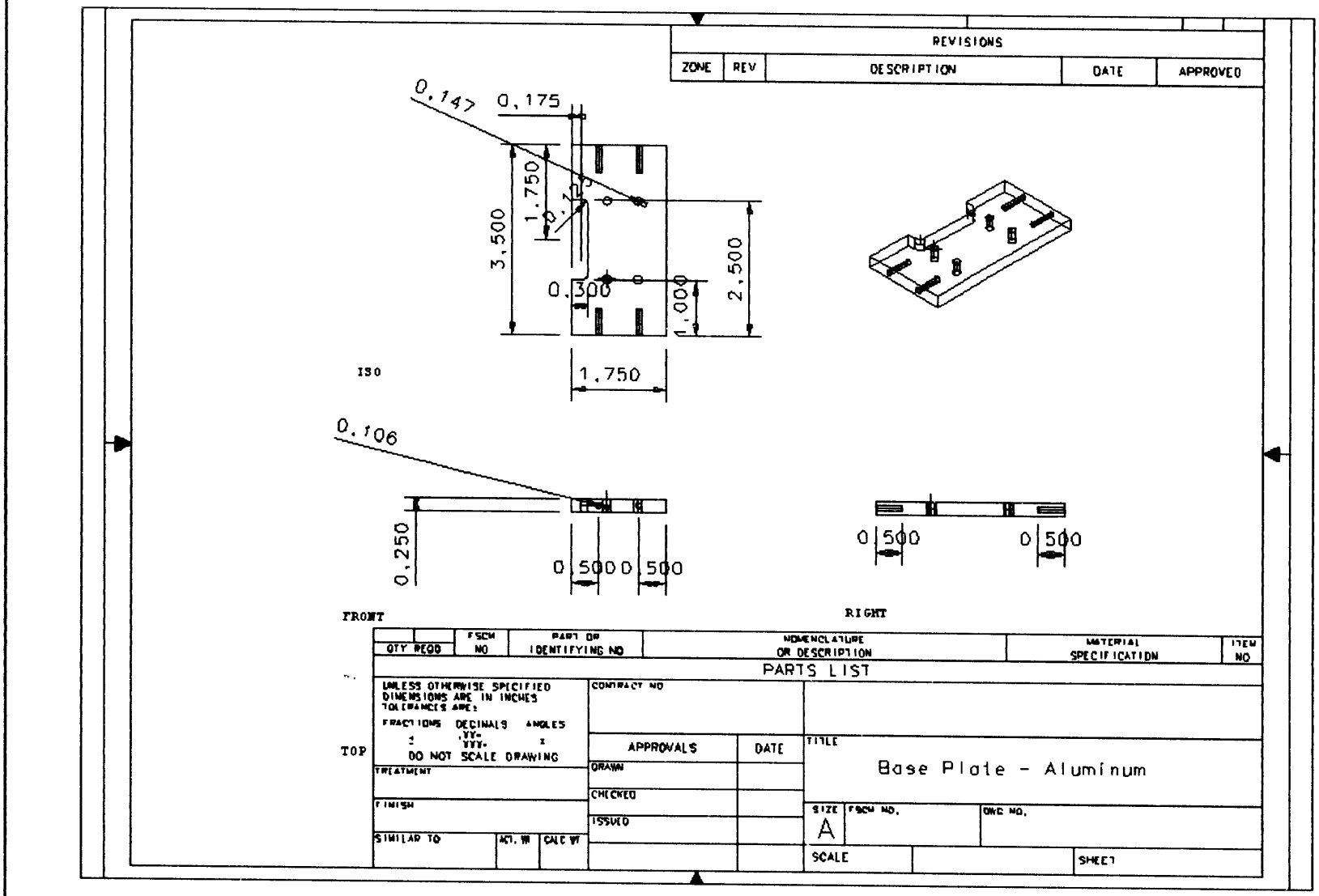
REVISIONS
ZONE
REV
DESCRIPTION
DATE
APPROVED
0.147
0.175
1.750
0.125
3.500
2.500
0.300
1.000
1.750
ISO
0.106
0.250
0.500
0.500
0.500
0.500
FRONT
RIGHT
QTY REQD
FSCM NO
PART OR IDENTIFYING NO
NOMENCLATURE OR DESCRIPTION
MATERIAL SPECIFICATION
ITEM NO
PARTS LIST
UNLESS OTHERWISE SPECIFIED DIMENSIONS ARE IN INCHES
TOLERANCES ARE:
FRACTIONS
DECIMALS
ANGLES
± .YY= .YYY= ±
DO NOT SCALE DRAWING
TOP
CONTRACT NO
APPROVALS
DATE
DRAWN
CHECKED
ISSUED
TREATMENT
FINISH
SIMILAR TO
MAT. WT
CALC WT
TITLE
Base Plate - Aluminum
SIZE
A
FSCM NO.
DWG NO.
SCALE
SHEET

DWG. NO.	SH	REV

REVISIONS

ZONE	REV	DESCRIPTION	DATE	APPROVED

7-BOTTOM

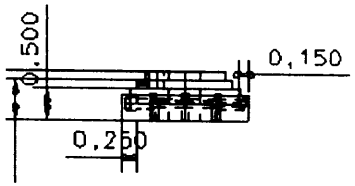

4-TOP

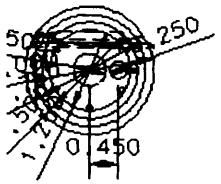

6-BACK

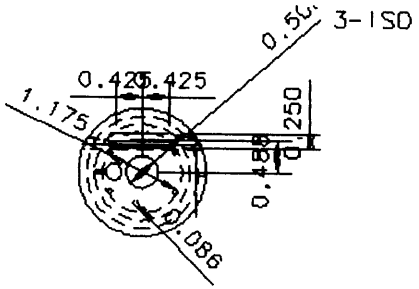

3-ISO

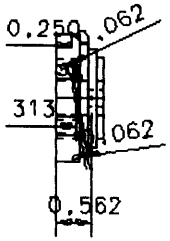

5-RIGHT

2-FRONT

QTY REQD	FSCM NO	PART OR IDENTIFYING NO	NOMENCLATURE OR DESCRIPTION	MATERIAL SPECIFICATION	ITEM NO

PARTS LIST

UNLESS OTHERWISE SPECIFIED DIMENSIONS ARE IN INCHES TOLERANCES ARE: FRACTIONS ± DECIMALS .XX± .XXX± ANGLES ± DO NOT SCALE DRAWING	CONTRACT NO	
TREATMENT	APPROVALS / DRAWN	DATE
FINISH	CHECKED	
SIMILAR TO / MAT'L / DWG NO	ISSUED	
		TITLE: 8-LEFT Differential - Aluminum
		SIZE A / FSCM NO. / DWG NO.
		SCALE / SHEET

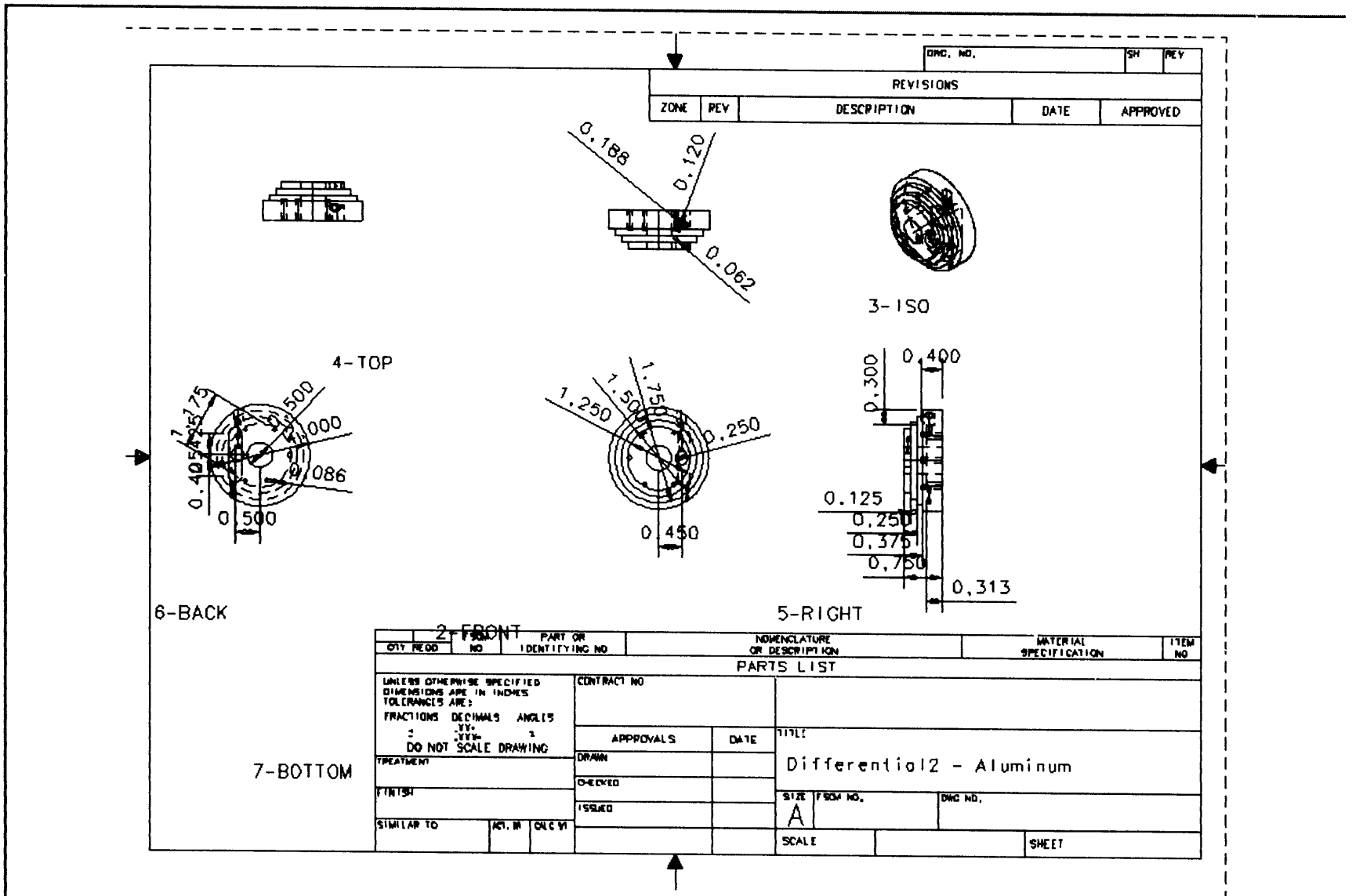
DWG. NO.
SH
REV
REVISIONS
ZONE
REV
DESCRIPTION
DATE
APPROVED
0.188
0.120
0.062
3-ISO
4-TOP
0.500
0.086
0.500
1.750
1.500
1.250
0.250
0.450
0.400
0.300
0.125
0.250
0.375
0.750
0.313
6-BACK
2-FRONT
5-RIGHT
QTY REQD
ITEM NO
PART OR IDENTIFYING NO
NOMENCLATURE OR DESCRIPTION
MATERIAL SPECIFICATION
ITEM NO
PARTS LIST
UNLESS OTHERWISE SPECIFIED DIMENSIONS ARE IN INCHES TOLERANCES ARE:
FRACTIONS DECIMALS ANGLES
DO NOT SCALE DRAWING
CONTRACT NO
APPROVALS
DATE
DRAWN
CHECKED
ISSUED
TREATMENT
FINISH
SIMILAR TO
MATL
CALC'N
TITLE
Differential2 - Aluminum
SIZE
A
FSCM NO.
DWG NO.
SCALE
SHEET
7-BOTTOM

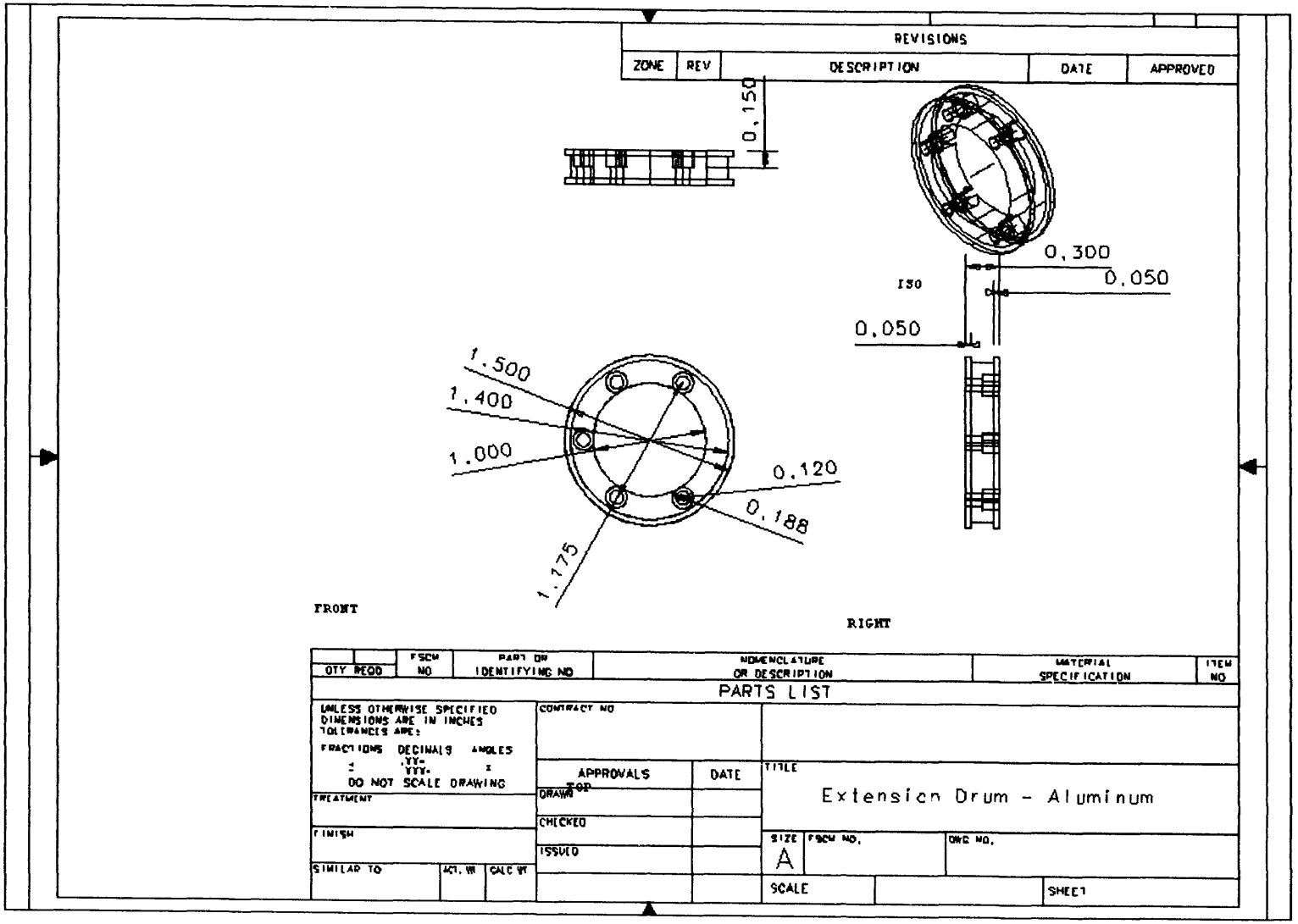
REVISIONS
ZONE
REV
DESCRIPTION
DATE
APPROVED
0.150
0.300
0.050
ISO
0.050
1.500
1.400
1.000
0.120
0.188
1.175
FRONT
RIGHT
QTY REQD
FSCM NO
PART OR IDENTIFYING NO
NOMENCLATURE OR DESCRIPTION
MATERIAL SPECIFICATION
ITEM NO
PARTS LIST
UNLESS OTHERWISE SPECIFIED DIMENSIONS ARE IN INCHES
TOLERANCES ARE:
FRACTIONS
DECIMALS .XX± .YYY±
ANGLES ±
DO NOT SCALE DRAWING
CONTRACT NO
APPROVALS
DATE
DRAWN
CHECKED
ISSUED
TREATMENT
FINISH
SIMILAR TO
MAT'L WT
CALC WT
TITLE
Extension Drum - Aluminum
SIZE
A
FSCM NO.
DWG NO.
SCALE
SHEET

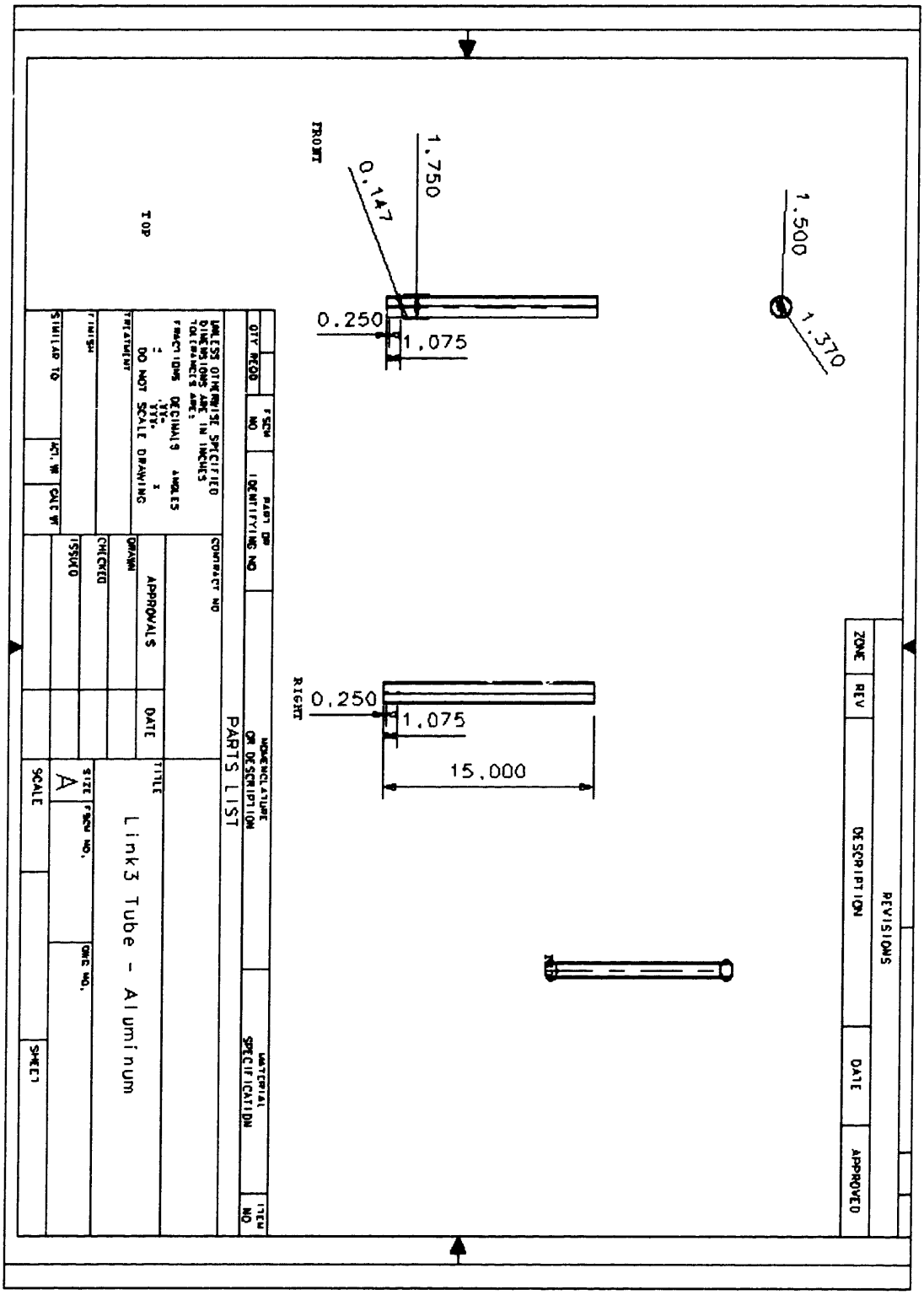
FRONT
1.750
0.147
0.250
1.075
1.500
1.370
RIGHT
0.250
1.075
15.000
TOP
REVISIONS
ZONE
REV
DESCRIPTION
DATE
APPROVED
UNLESS OTHERWISE SPECIFIED
DIMENSIONS ARE IN INCHES
TOLERANCES ARE:
FRACTIONS DECIMALS ANGLES
DO NOT SCALE DRAWING
QTY REQD
FSCM NO
IDENTIFYING NO
NOMENCLATURE OR DESCRIPTION
MATERIAL SPECIFICATION
ITEM NO
CONTRACT NO
APPROVALS
DRAWN
CHECKED
ISSUED
DATE
PARTS LIST
FINISH
TREATMENT
MATERIAL TO
SIMILAR TO
NEXT ASSY
USED ON
TITLE
Link3 Tube - Aluminum
SIZE
A
FSCM NO.
DWG NO.
SCALE
SHEET

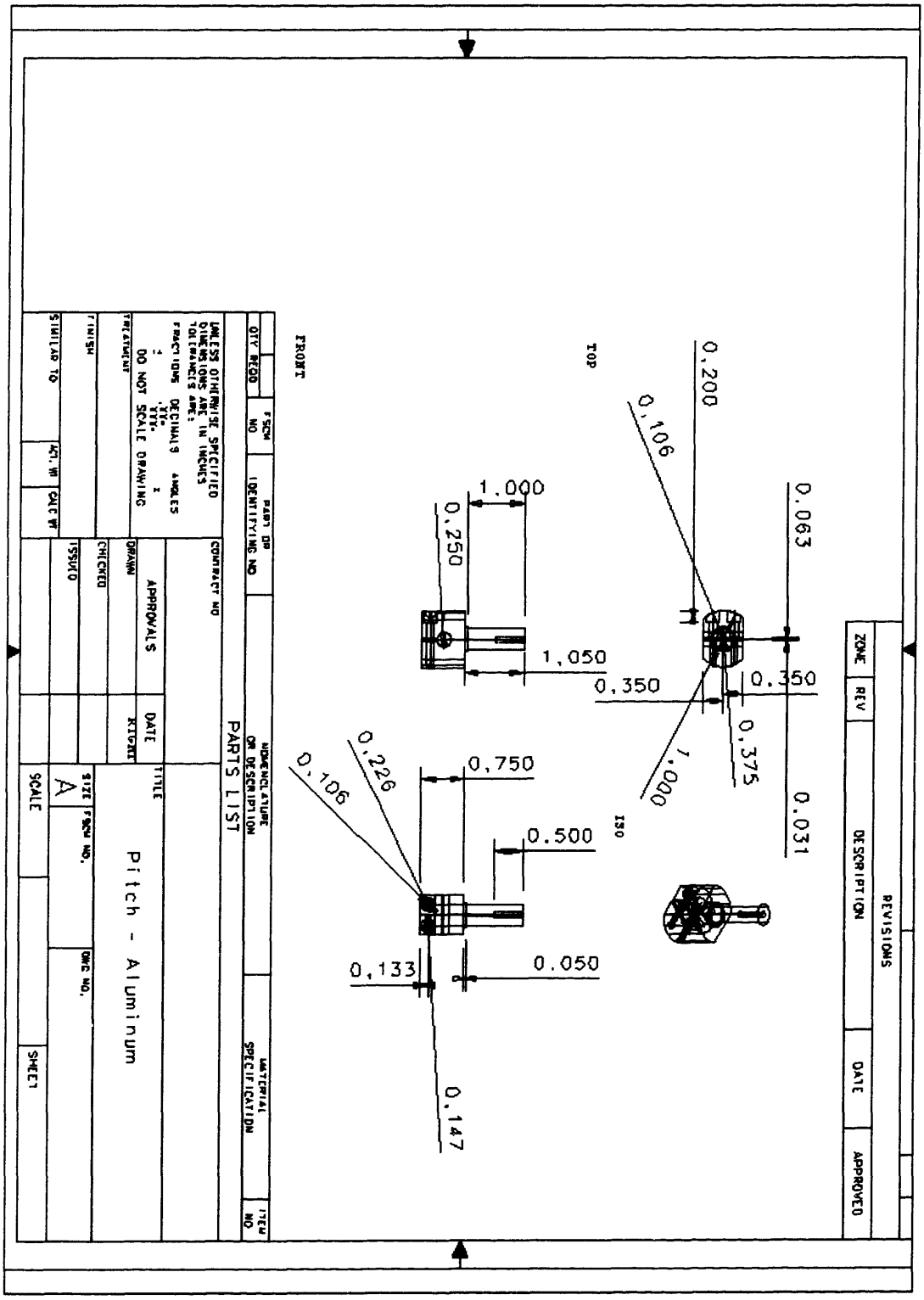
FRONT
TOP
ISO
0.200
0.106
0.063
1.000
0.250
1.050
0.350
0.350
0.375
1.000
0.031
0.750
0.226
0.106
0.500
0.133
0.050
0.147
REVISIONS
ZONE
REV
DESCRIPTION
DATE
APPROVED
PARTS LIST
ITEM NO
MATERIAL SPECIFICATION
NOMENCLATURE OR DESCRIPTION
PART ID IDENTIFYING NO
QTY REQD
FSCM NO
CONTRACT NO
APPROVALS
DRAWN
CHECKED
ISSUED
TREATMENT
FINISH
SIMILAR TO
NEXT ASY
CALC WT
DO NOT SCALE DRAWING
UNLESS OTHERWISE SPECIFIED DIMENSIONS ARE IN INCHES TOLERANCES ARE: FRACTIONS DECIMALS ANGLES
Pitch - Aluminum
SIZE
A
FSCM NO.
DWG NO.
SCALE
SHEET

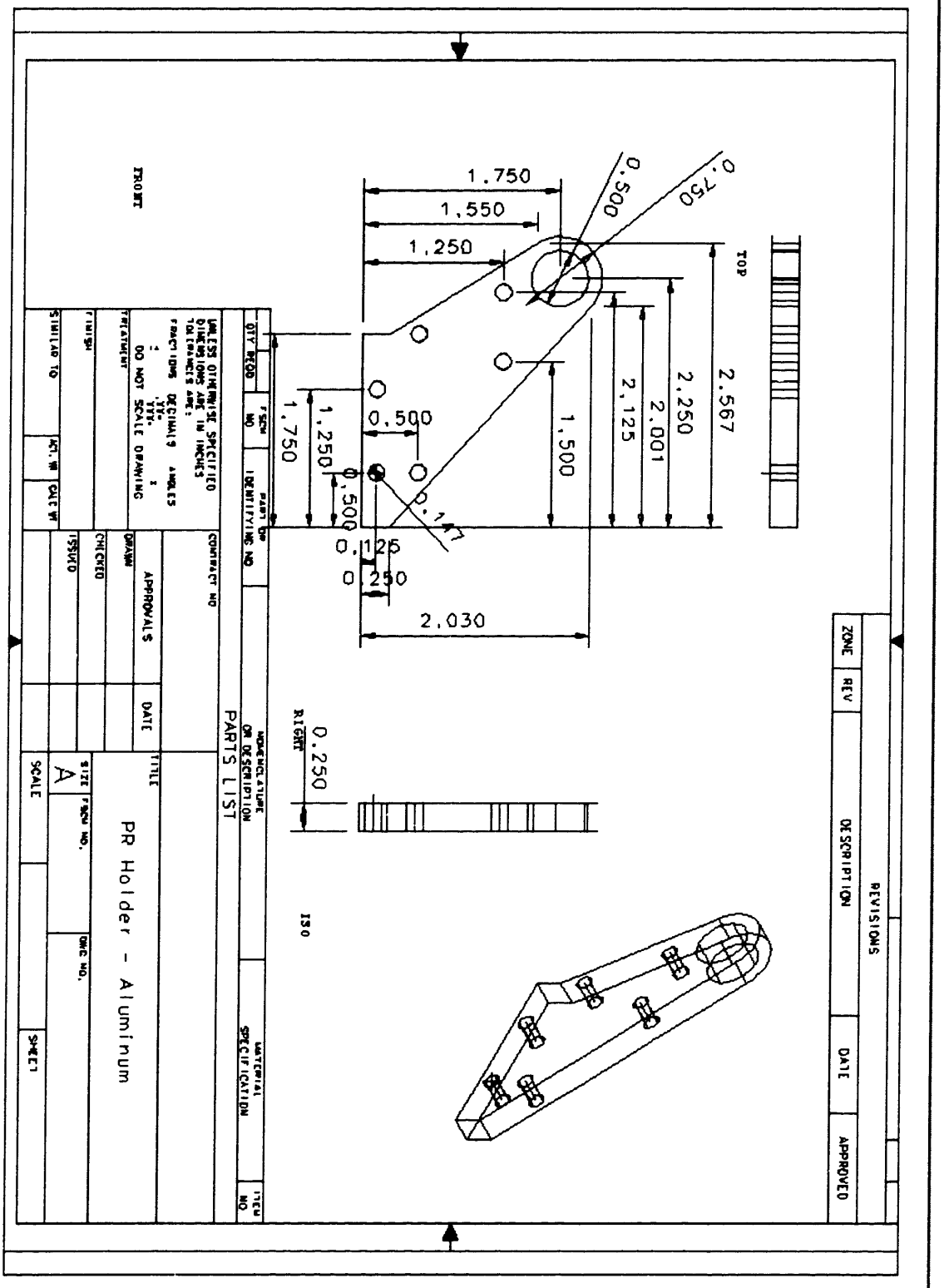
FRONT
TOP
RIGHT
ISO
1.750
1.550
1.250
0.500
0.750
2.567
2.250
2.001
2.125
1.500
1.750
1.250
0.500
0.500
0.125
0.250
2.030
0.250
REVISIONS
ZONE
REV
DESCRIPTION
DATE
APPROVED
PARTS LIST
PR Holder - Aluminum
SCALE
SHEET
SIZE
A

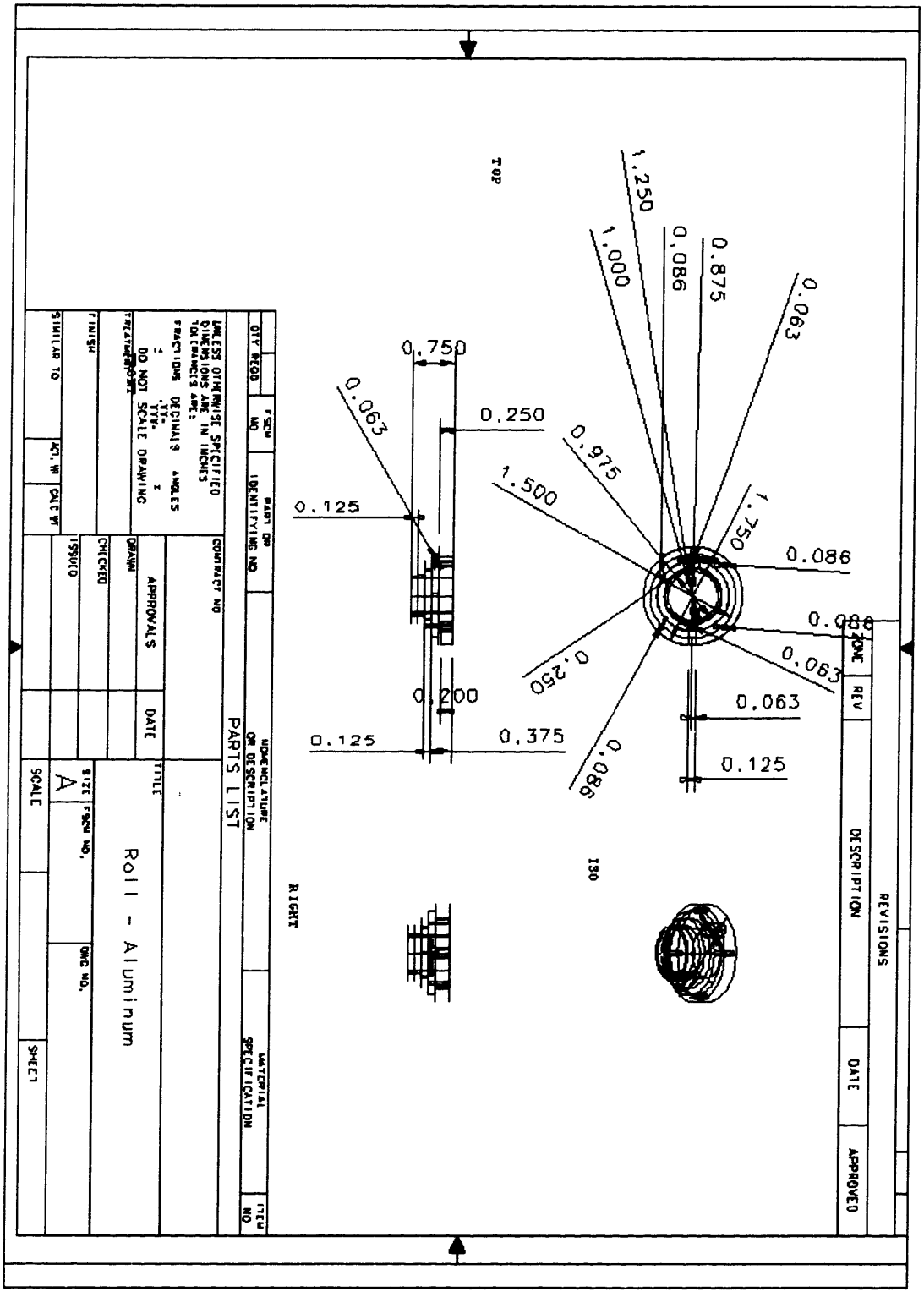
TOP
RIGHT
ISO
1.250
1.000
0.086
0.875
0.063
0.750
0.063
0.250
0.975
1.500
0.125
1.750
0.086
0.063
0.250
0.200
0.063
0.125
0.375
0.086
0.125
REVISIONS
ZONE
REV
DESCRIPTION
DATE
APPROVED
UNLESS OTHERWISE SPECIFIED
DIMENSIONS ARE IN INCHES
TOLERANCES ARE:
FRACTIONS DECIMALS ANGLES
.XX±
.XXX±
DO NOT SCALE DRAWING
QTY. REQD
FSCM NO
PART OR IDENTIFYING NO.
NOMENCLATURE OR DESCRIPTION
MATERIAL SPECIFICATION
ITEM NO
CONTRACT NO
APPROVALS
DATE
DRAWN
CHECKED
ISSUED
PARTS LIST
FINISH
SIMILAR TO
NEXT ASSY
USED ON
SCALE
WT.
SHEET
SIZE
A
FSCM NO.
DWG NO.
TITLE
Roll - Aluminum

REVISIONS				
ZONE	REV	DESCRIPTION	DATE	APPROVED

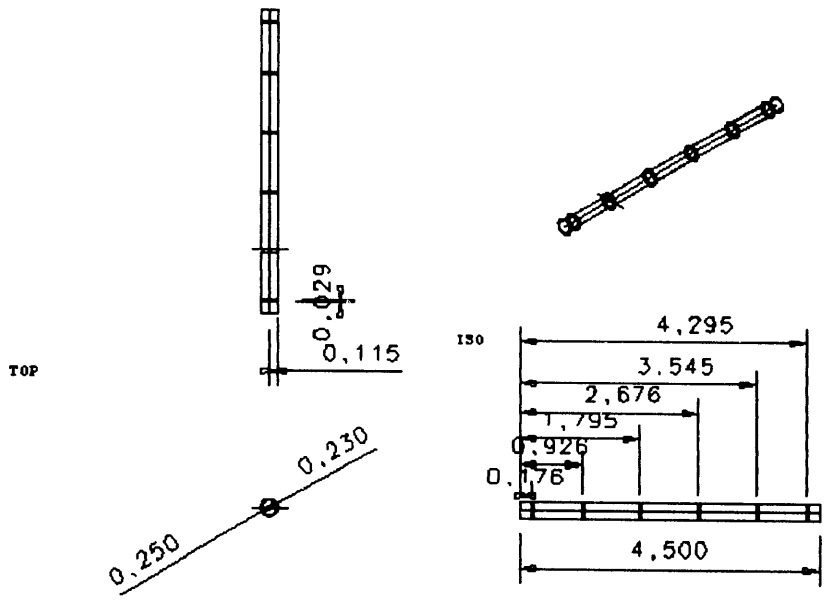

QTY REQD	FSCM NO	PART OR IDENTIFYING NO	NOMENCLATURE OR DESCRIPTION	MATERIAL SPECIFICATION	ITEM NO

PARTS LIST

UNLESS OTHERWISE SPECIFIED
DIMENSIONS ARE IN INCHES
TOLERANCES ARE:
FRACTIONS ± DECIMALS .XX± .XXX± ANGLES ±
DO NOT SCALE DRAWING

TREATMENT

FINISH

SIMILAR TO | MAT. W | CALC W

CONTRACT NO

APPROVALS	DATE
DRAWN	
CHECKED	
ISSUED	

RIGHT

TITLE
Shaft - Stainless Steel

SIZE A | FSCM NO. | DWG NO.

SCALE | SHEET

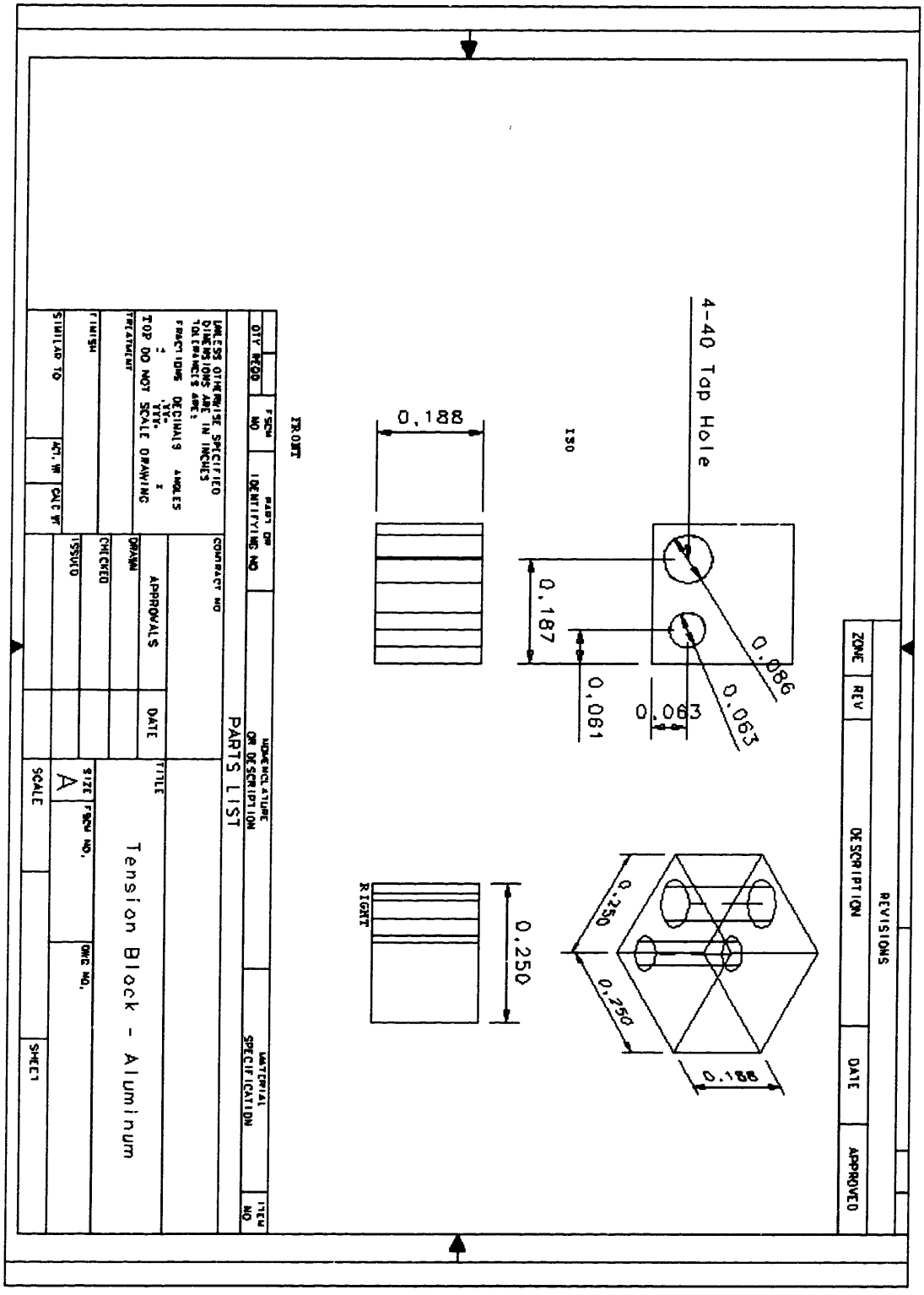
4-40 Tap Hole
ISO
FRONT
RIGHT
0.188
0.187
0.086
0.063
0.063
0.061
0.250
0.250
0.188
REVISIONS
ZONE
REV
DESCRIPTION
DATE
APPROVED
PARTS LIST
Tension Block - Aluminum
SIZE
A
SCALE
SHEET

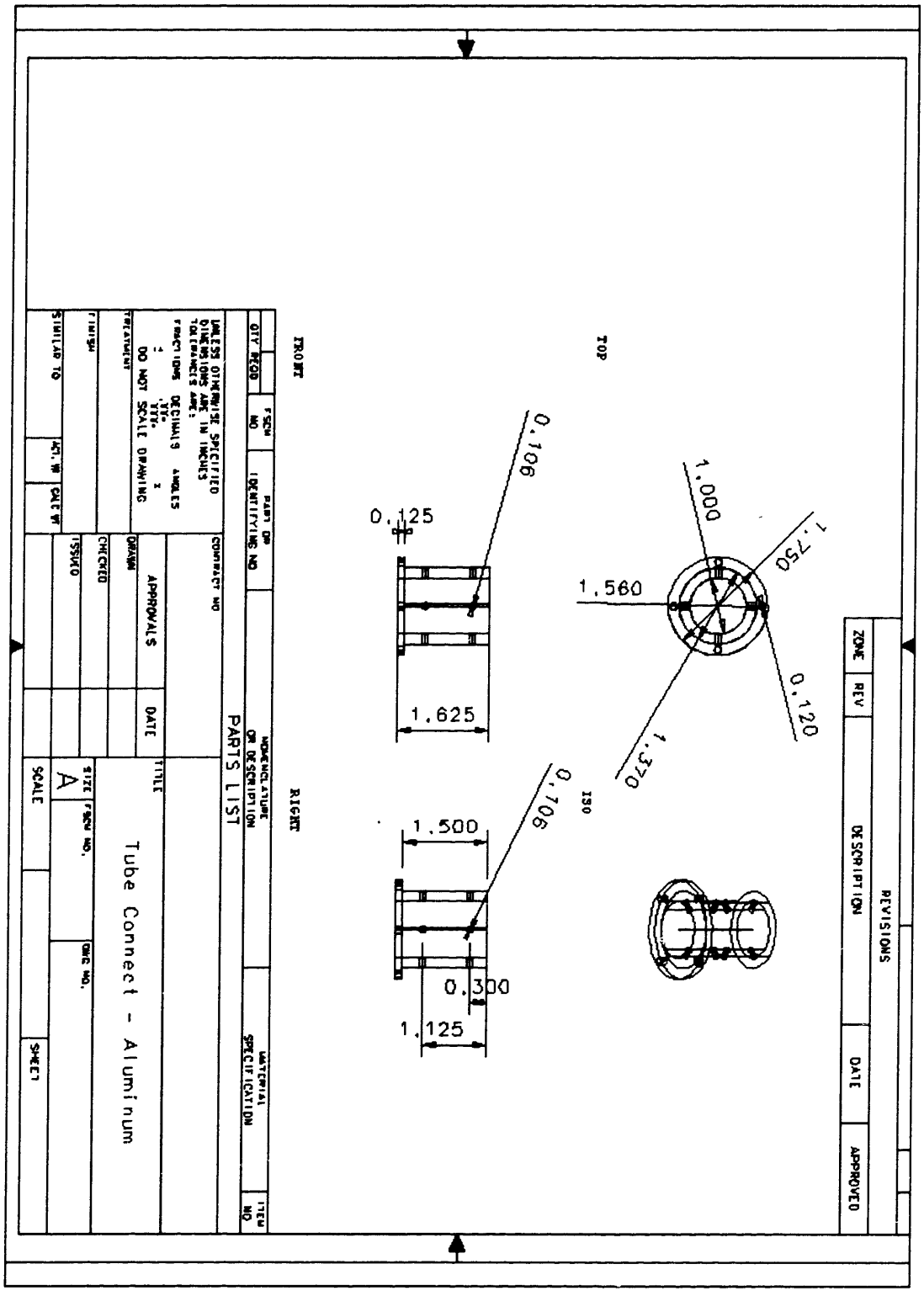
FRONT
TOP
RIGHT
ISO
0.125
0.106
1.625
1.500
0.300
1.125
1.560
1.000
1.750
0.120
1.370
0.106
PARTS LIST
Tube Connect - Aluminum
REVISIONS

THESIS PROCESSING SLIP

FIXED FIELD: ill. _____ name _____

index _____ biblio _____

▶ COPIES: (Archives) Aero Dewey (Eng) Hum
Lindgren Music Rotch Science

TITLE VARIES: ▶ ☑ Arms

NAME VARIES: ▶ ☐ _____

IMPRINT: (COPYRIGHT) _____

▶ COLLATION: 81 P

▶ ADD: DEGREE: _____ ▶ DEPT.: _____

SUPERVISORS: _____

NOTES:

cat'r: date:

page: 531

▶ DEPT: M.E.

▶ YEAR: 1999 ▶ DEGREE: S.M.

▶ NAME: KATZ, Arrin